Multi-scale modelling of calcification in cnidarians

Jaap A. Kaandorp
Computational Science Lab
Faculty of Science
University of Amsterdam
Science Park 904, 1098 XH Amsterdam
The Netherlands
E-mail: J.A.Kaandorp@uva.nl
http://www.science.uva.nl/~jaapk

From DNA to Form

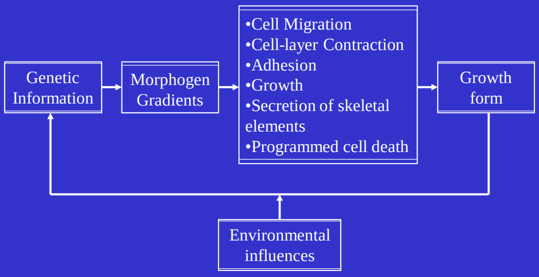

Genetic Information

Morphogen Gradients

- Cell Migration
- Cell-layer Contraction
- Adhesion
- Growth
- Secretion of skeletal elements
- Programmed cell death

Growth form

Environmental influences

The animal kingdom

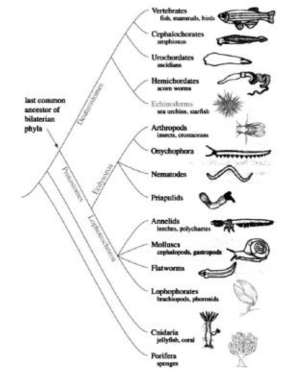

Nematostella vectensis (top) / *Acropora millepora* (bottom) (Ball et al., Nature Reviews Genetics: 567, 2004)

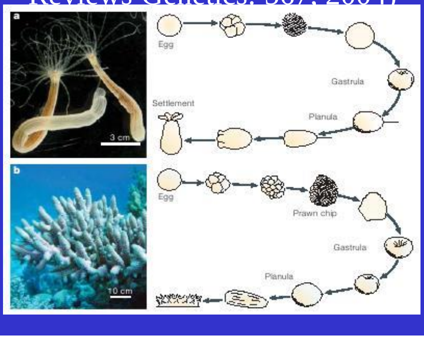

Growth of corals: a multiscale problem

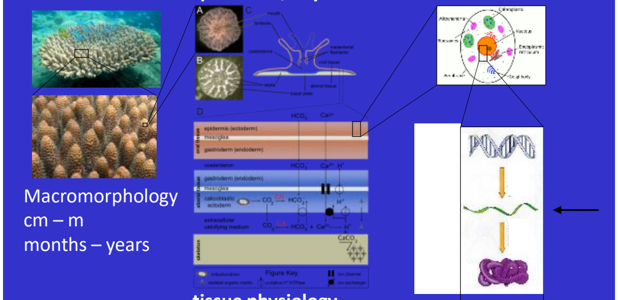

Micromorphology
µm – mm; days - weeks

cell physiology
1 – 10 µm; ns - hours

Macromorphology
cm – m
months – years

tissue physiology
1 – 100 µm; ns -µs

molecular physiology
Å – nm; s - mins

Overview

- Modelling gene regulation
- The sea anemone *Nematostella vectensis* case study modelling gene regulation
- Cell-based modelling of gastrulation in *Nematostella* and the hydrozoan *Clytia hemisphaerica*
- Biomineralisation in the scleractinian coral *Acropora millepora*
- Modelling calcification physiology in corals
- Modelling growth and form of corals (e.g *Madracis sp.*) and the impact of the physical environment

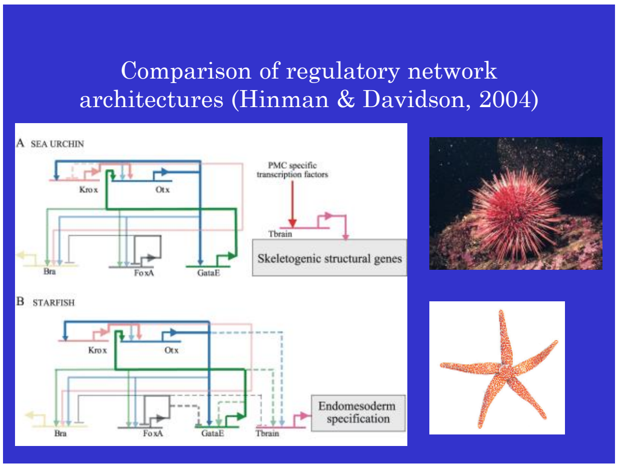

Comparison of regulatory network architectures (Hinman & Davidson, 2004)

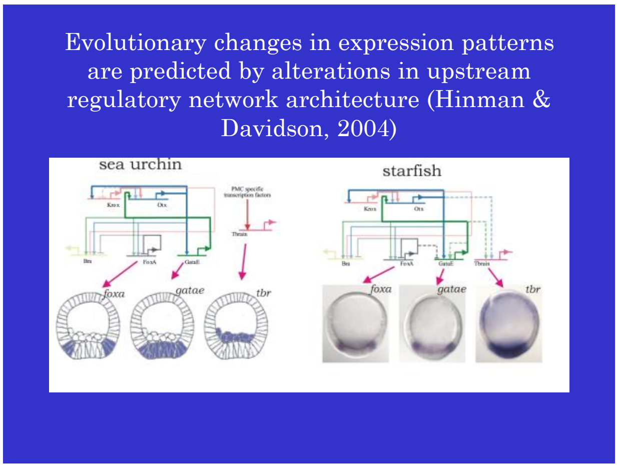

Evolutionary changes in expression patterns are predicted by alterations in upstream regulatory network architecture (Hinman & Davidson, 2004)

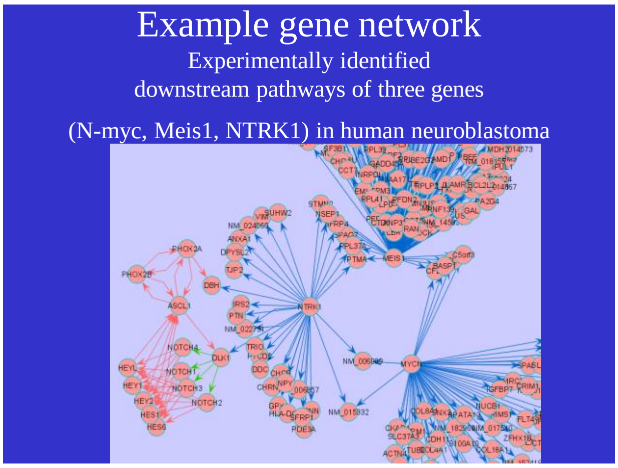

Example gene network

Experimentally identified
downstream pathways of three genes

(N-myc, Meis1, NTRK1) in human neuroblastoma

Possible components in a gene network model

- Forward flow of information from gene to mRNA to protein
- Positive and negative feedback loops
- Information exchange with metabolic pathways, signalling pathways
- Biomechanics of cells
- Spatial component

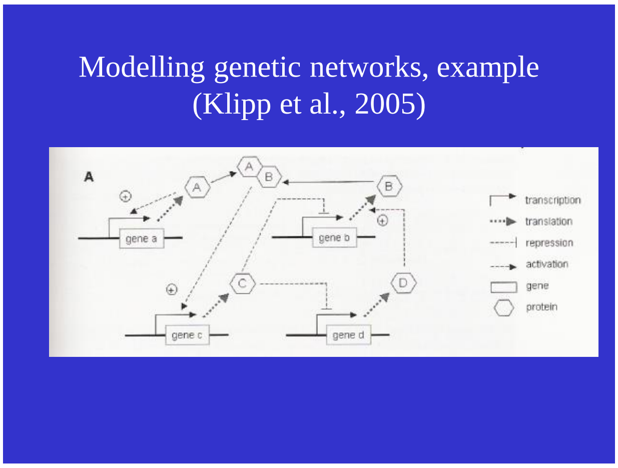

Modelling genetic networks, example (Klipp et al., 2005)

Different models for gene networks

- Boolean networks
- Ordinary differential equations
- Partial differential equations
- …

Genetic networks: the major challenges

- Understanding the dynamics and how gene networks regulate processes is a major (not solved in general) challenge! How do we model such a network? Complication: regulatory networks are very large, many details (needed in the models) are frequently missing
- major challenge: how to infer regulatory networks from gene expression data? How to infer model parameters?
- Major challenge: how do we couple models of regulatory networks and biomechanical models (for example models of growth and development)?

Modelling genetic networks, example

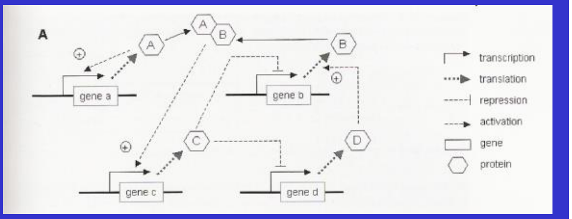

Modelling genetic networks with ODEs

$$\frac{dx_i}{dt} = f_i(x_1,\ldots,x_n), i = 1,\ldots,n$$

- Where x_i represent the concentrations of mRNAs, proteins, or other molecules and n number of genes

Modelling genetic networks with ODEs, example II

- Consider only mRNA quantities a,b,c and d:

$$\frac{da}{dt} = f_a(a)$$
$$\frac{db}{dt} = f_b(b,c,d)$$
$$\frac{dc}{dt} = f_a(a,b,c)$$
$$\frac{dd}{dt} = f_d(c,d)$$

Modelling enzyme kinetics

- Binding of ligands to proteins, case binding of n ligands (S) to a protein (E), complete cooperativity (Hill equation)

$$v = \frac{V_{\max} K_B S^n}{1 + K_B S^n}$$

Hill function

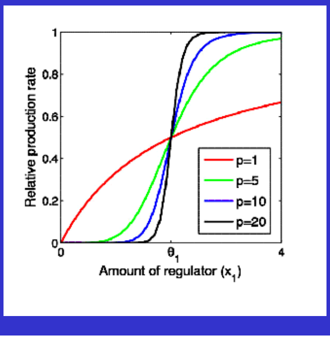

Modelling genetic networks with ODEs, example III

- A possible model of the regulatory network describing quantities of mRNA:

$$\frac{da}{dt} = v_a - k_a \cdot a$$
$$\frac{db}{dt} = \frac{V_b \cdot d^{n_d}}{(K_b + d^{n_d})(K_{Ic} + c^{n_c})} - k_b \cdot b$$
$$\frac{dc}{dt} = \frac{V_c \cdot (a \cdot b)^{n_{ab}}}{K_c + (a \cdot b)^{n_{ab}}} - k_c \cdot c$$
$$\frac{dd}{dt} = \frac{V_d}{K_{Ic} + c^{n_c}} - k_d \cdot d$$

- Here k_a,k_b,k_c,k_d are rate constants of the degradation of a,b,c and d. v_a is a constant rate of expression

Modelling genetic networks with ODEs, example III

- A possible model of the regulatory network describing quantities of mRNA:

$$\frac{da}{dt} = v_a - k_a \cdot a$$
$$\frac{db}{dt} = \frac{V_b \cdot d^{n_d}}{(K_b + d^{n_d})(K_{Ic} + c^{n_c})} - k_b \cdot b$$
$$\frac{dc}{dt} = \frac{V_c \cdot (a \cdot b)^{n_{ab}}}{K_c + (a \cdot b)^{n_{ab}}} - k_c \cdot c$$
$$\frac{dd}{dt} = \frac{V_d}{K_{Ic} + c^{n_c}} - k_d \cdot d$$

$\frac{V_b \cdot d^{n_d}}{(K_b + d^{n_d})}$ Is Hill term with Max rate V_b, Dissociation constant K_b and Hill coefficient n_d

$(K_{Ic} + c^{n_c})$ Is inhibition term

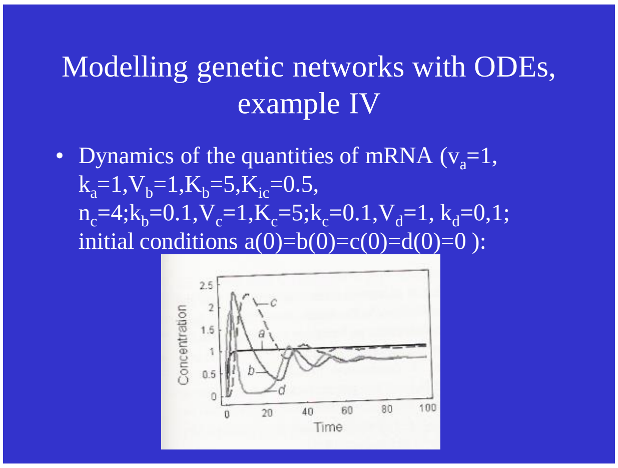

Modelling genetic networks with ODEs, example IV

- Dynamics of the quantities of mRNA (v_a=1, k_a=1,V_b=1,K_b=5,K_{ic}=0.5, n_c=4;k_b=0.1,V_c=1,K_c=5;k_c=0.1,V_d=1, k_d=0,1; initial conditions a(0)=b(0)=c(0)=d(0)=0):

Modelling genetic networks with ODEs

- Advantage: can take into account detailed knowledge about regulatory network (including quantitative information; temporal information for example time delays, slow and fast processes; can be extended to PDE description including spatial information)
- Disadvantage: current lack of this detailed knowledge! Many parameters are not available, you need an additional method to estimate these parameters from actual data.
- Disadvantage: the ODE description is a macroscopic one, in many steps only a few molecules are involved.
- Disadvantage: no spatial component

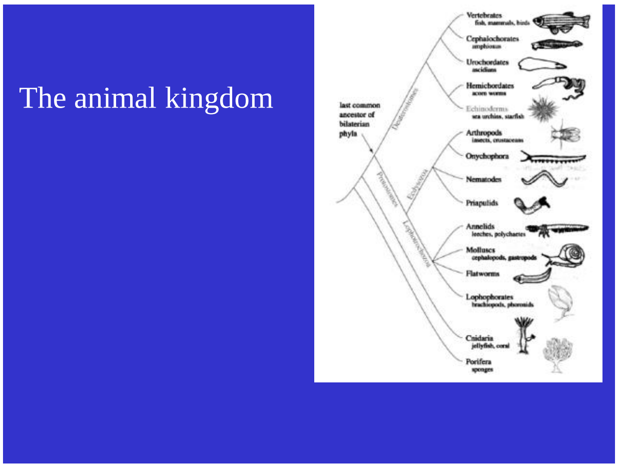

The animal kingdom

- Reconstruction of gene regulatory networks in *Nematostella vectensis*, (Botman & Kaandorp, BMC Research Notes, 2012; Abdol et al. Dev. Biol. 2017)

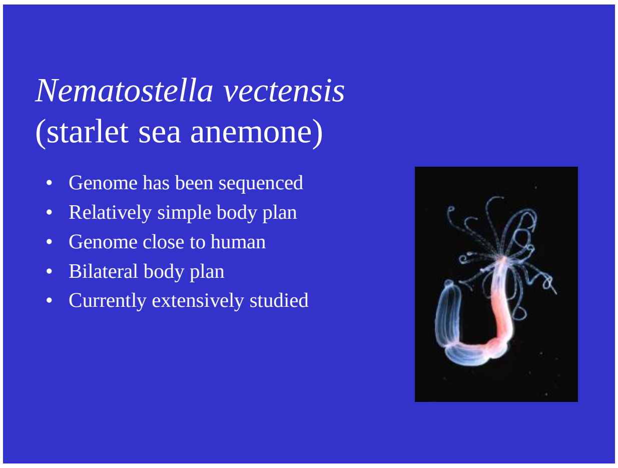

Nematostella vectensis (starlet sea anemone)

- Genome has been sequenced
- Relatively simple body plan
- Genome close to human
- Bilateral body plan
- Currently extensively studied

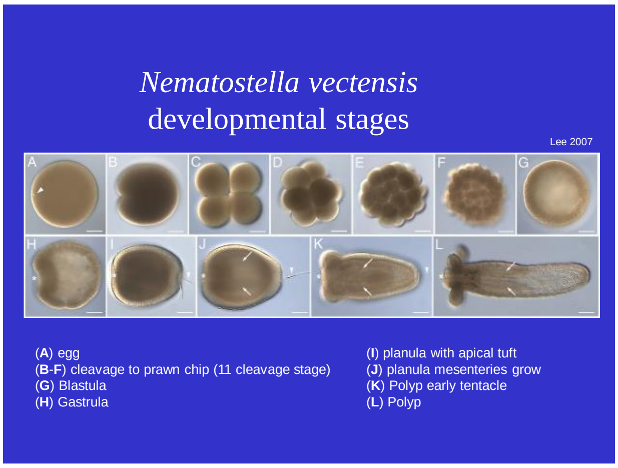

Nematostella vectensis developmental stages

Lee 2007

(A) egg
(B-F) cleavage to prawn chip (11 cleavage stage)
(G) Blastula
(H) Gastrula
(I) planula with apical tuft
(J) planula mesenteries grow
(K) Polyp early tentacle
(L) Polyp

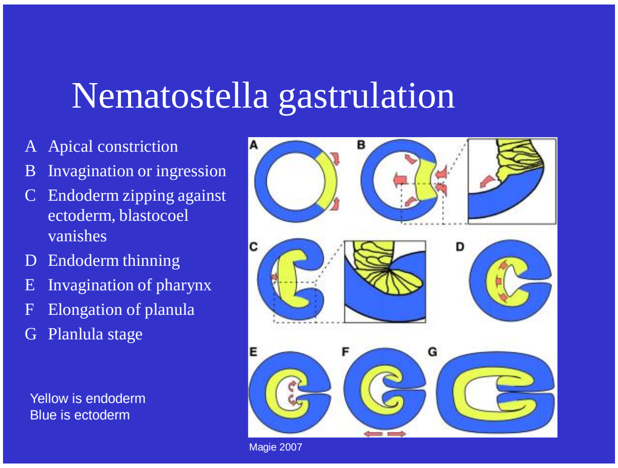

Nematostella gastrulation

A Apical constriction
B Invagination or ingression
C Endoderm zipping against ectoderm, blastocoel vanishes
D Endoderm thinning
E Invagination of pharynx
F Elongation of planula
G Planlula stage

Yellow is endoderm
Blue is ectoderm

Magie 2007

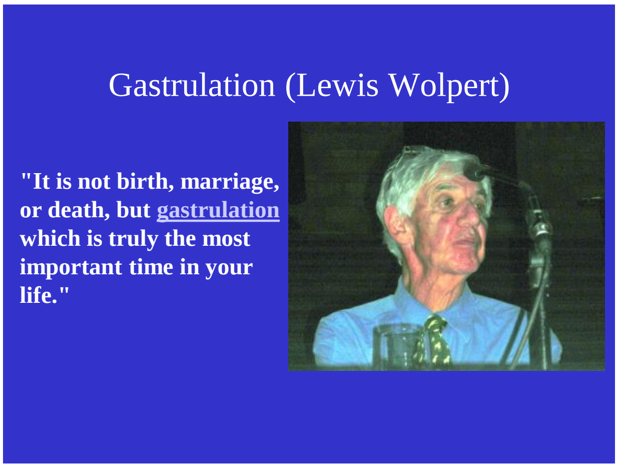

Gastrulation (Lewis Wolpert)

"It is not birth, marriage, or death, but gastrulation which is truly the most important time in your life."

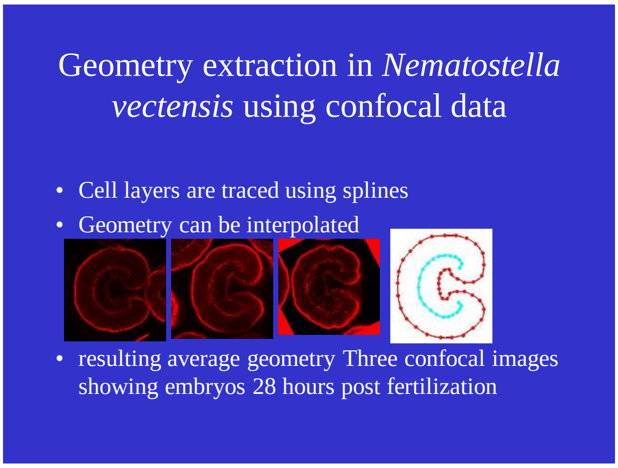

Geometry extraction in *Nematostella vectensis* using confocal data

- Cell layers are traced using splines
- Geometry can be interpolated
- resulting average geometry Three confocal images showing embryos 28 hours post fertilization

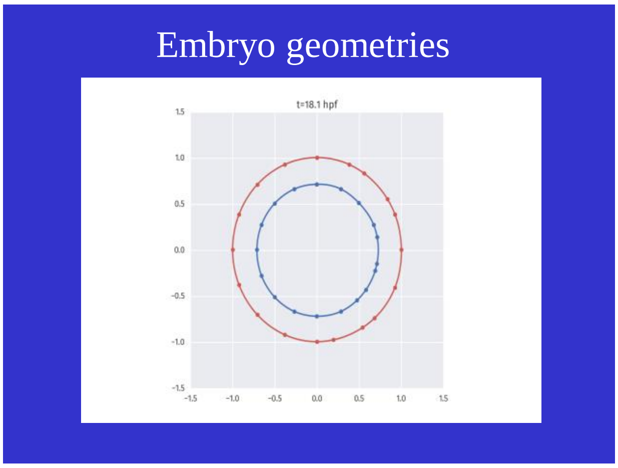

Embryo geometries

Developmental genes and signalling pathways in *Acropora millepora* and *Nematostella vectensis*

- Transpcription factors (within cell nucleus)
  - Homeobox genes
  - Sox genes
  - Fox genes
  - Other genes
- Wnt signalling pathway (diffusable ligands)
- TGF beta signalling pathway (diffusable ligands)
- FGF signalling pathway (diffusable ligands)
- ...

: data base *Nematostella vectensis* gene expression patterns (in situ data Kahi Kai data base) I

- The name of the gene
- The developmental phase during which the expression was observed
- The location where the expression was observed The level of expression A reference to a scientific publication An image of the gene expression pattern
- The assay type used for the image, usually in situ hybridization
- A verbal description of the gene expression pattern
- Other possible remarks

Choose Relevant Genes

- NemaBase: 105 genes; >800 expression patterns
- Criteria first selection:
  - AP expression
  - Upto late gastrula
  - AP 'functional module'

Final list of genes. For this resulting set of genes quantifications were made for early developmental stages (up to mid gastrula)

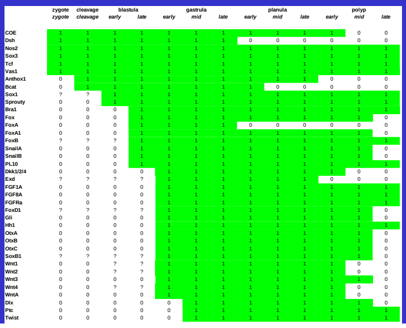

	zygote	cleavage	blastula		gastrula			planula			polyp		
	zygote	*cleavage*	*early*	*late*	*early*	*mid*	*late*	*early*	*mid*	*late*	*early*	*mid*	*late*
COE	1	1	1	1	1	1	1	1	1	1	1	0	0
Dsh	1	1	1	1	1	1	1	0	0	0	0	0	0
Nos2	1	1	1	1	1	1	1	1	1	1	1	1	1
Sox3	1	1	1	1	1	1	1	1	1	1	1	1	1
Tcf	1	1	1	1	1	1	1	1	1	1	1	1	1
Vas1	1	1	1	1	1	1	1	1	1	1	1	1	1
Anthox1	0	1	1	1	1	1	1	1	1	1	0	0	0
Bcat	0	1	1	1	1	1	1	1	0	0	0	0	0
Sox1	?	?	1	1	1	1	1	1	1	1	1	1	1
Sprouty	0	0	1	1	1	1	1	1	1	1	1	1	1
Bra1	0	0	0	1	1	1	1	1	1	1	1	1	1
Fox	0	0	0	1	1	1	1	1	1	1	1	1	0
FoxA	0	0	0	1	1	1	1	0	0	0	0	0	0
FoxA1	0	0	0	1	1	1	1	1	1	1	1	1	0
FoxB	?	?	?	1	1	1	1	1	1	1	1	1	1
SnailA	0	0	0	1	1	1	1	1	1	1	1	1	0
SnailB	0	0	0	1	1	1	1	1	1	1	1	1	0
PL10	0	0	0	1	1	1	1	1	1	1	1	1	1
Dkk1/2/4	0	0	0	0	1	1	1	1	1	1	1	0	0
Exd	?	?	?	?	1	1	1	1	1	1	0	0	0
FGF1A	0	0	0	0	1	1	1	1	1	1	1	1	1
FGF8A	0	0	0	0	1	1	1	1	1	1	1	1	1
FGFRa	0	0	0	0	1	1	1	1	1	1	1	1	1
FoxD1	?	?	?	?	1	1	1	1	1	1	1	1	0
Gli	0	0	0	0	1	1	1	1	1	1	1	1	0
Hh1	0	0	0	0	1	1	1	1	1	1	1	1	1
OtxA	0	0	0	0	1	1	1	1	1	1	1	1	0
OtxB	0	0	0	0	1	1	1	1	1	1	1	1	0
OtxC	0	0	0	0	1	1	1	1	1	1	1	1	0
SoxB1	?	?	?	?	1	1	1	1	1	1	1	1	0
Wnt1	0	0	?	?	1	1	1	1	1	1	1	0	0
Wnt2	0	0	?	?	1	1	1	1	1	1	1	0	0
Wnt3	0	0	0	0	1	1	1	1	1	1	1	1	0
Wnt4	0	0	?	?	1	1	1	1	1	1	1	0	0
WntA	0	0	0	0	1	1	1	1	1	1	1	0	0
Dlx	0	0	0	0	0	1	1	1	1	1	1	1	0
Ptc	0	0	0	0	0	1	1	1	1	1	1	1	1
Twist	0	0	0	0	0	1	1	1	1	1	1	1	1

Quantify Expression Patterns

- **Load gene expression picture**
- **Choose stage**
- **Adjust geometry to fit the real embryo shape**
- **Perform decomposition**
- **Calculate expression levels**
- **Plot the expression profile**
- **Process the data, i.e. shift, scale, reduce noise etc.**
- **Combine all patterns of the genes of interest**

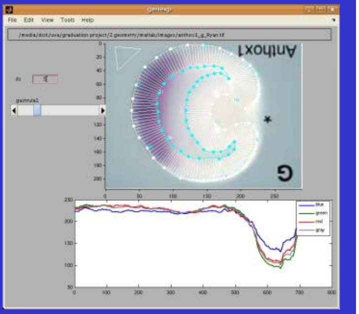

Quantify Expression Patterns

- **For selected genes**
- **If available (mostly 1 or 2 available)**
- **For relevant developmental stages**

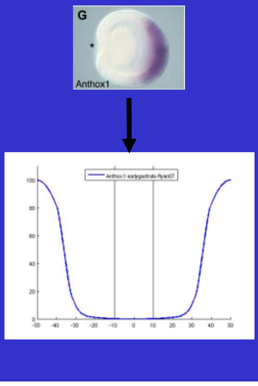

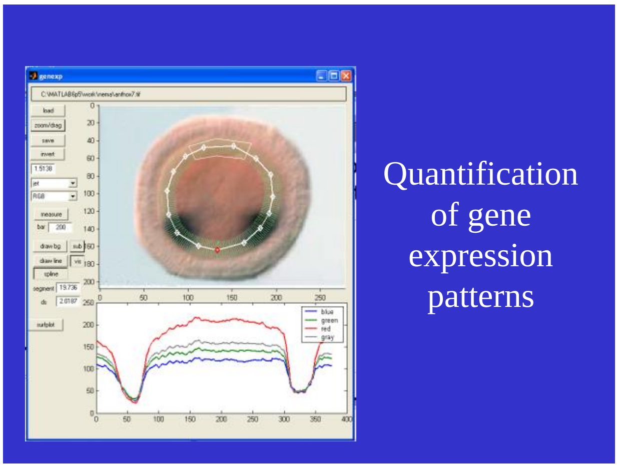

Quantification of gene expression patterns

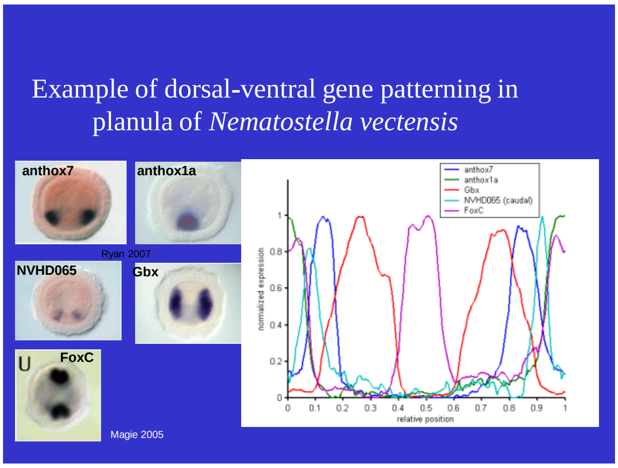

Example of dorsal-ventral gene patterning in planula of *Nematostella vectensis*

Ryan 2007

Magie 2005

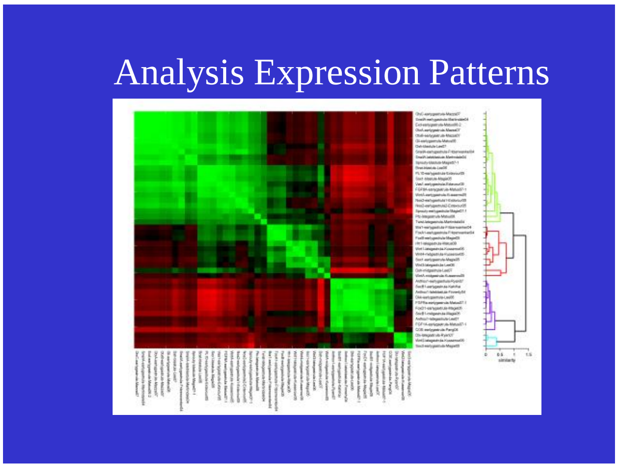

Analysis Expression Patterns

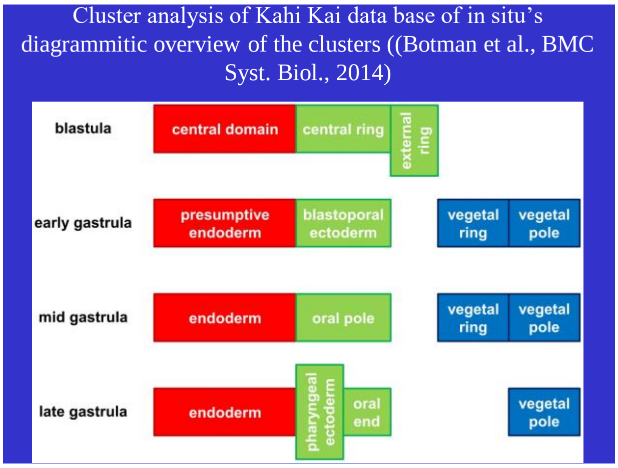

Cluster analysis of Kahi Kai data base of in situ's diagrammitic overview of the clusters ((Botman et al., BMC Syst. Biol., 2014)

blastula: central domain | central ring | external ring

early gastrula: presumptive endoderm | blastoporal ectoderm | vegetal ring | vegetal pole

mid gastrula: endoderm | oral pole | vegetal ring | vegetal pole

late gastrula: endoderm | pharyngeal ectoderm | oral end | vegetal pole

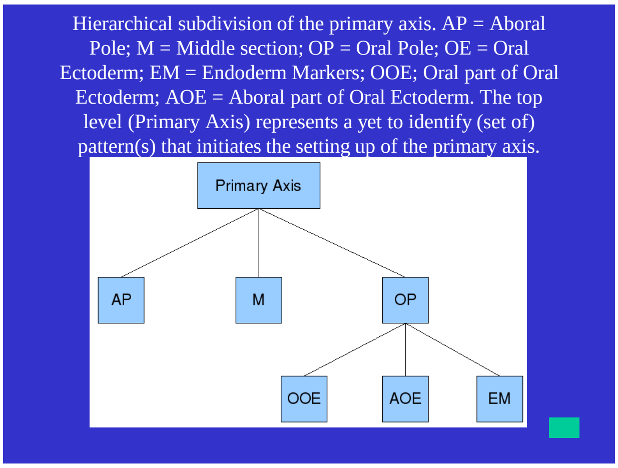

Hierarchical subdivision of the primary axis. AP = Aboral Pole; M = Middle section; OP = Oral Pole; OE = Oral Ectoderm; EM = Endoderm Markers; OOE; Oral part of Oral Ectoderm; AOE = Aboral part of Oral Ectoderm. The top level (Primary Axis) represents a yet to identify (set of) pattern(s) that initiates the setting up of the primary axis.

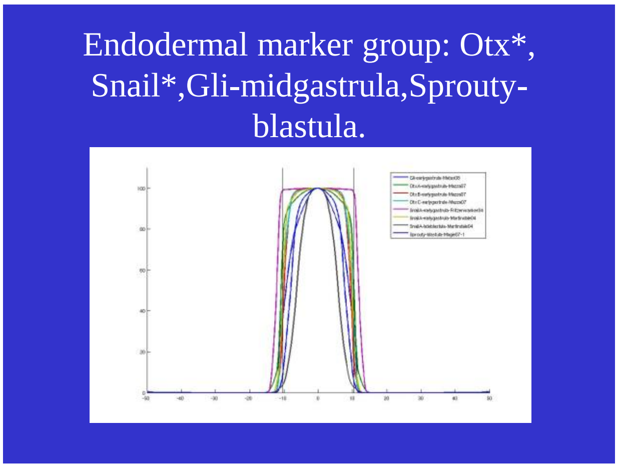

Endodermal marker group: Otx*, Snail*,Gli-midgastrula,Sprouty-blastula.

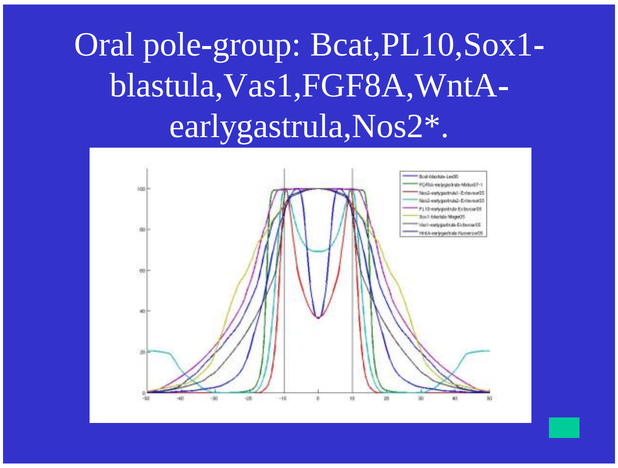

Oral pole-group: Bcat,PL10,Sox1-blastula,Vas1,FGF8A,WntA-earlygastrula,Nos2*.

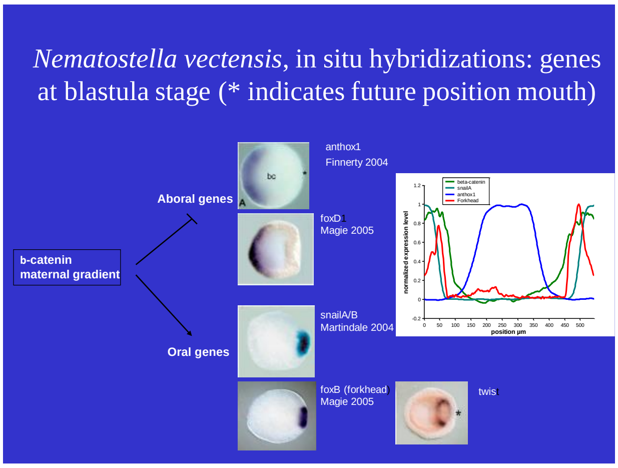

Nematostella vectensis, in situ hybridizations: genes at blastula stage (* indicates future position mouth)

b-catenin maternal gradient

Aboral genes

Oral genes

anthox1
Finnerty 2004

foxD1
Magie 2005

snailA/B
Martindale 2004

foxB (forkhead)
Magie 2005

twist

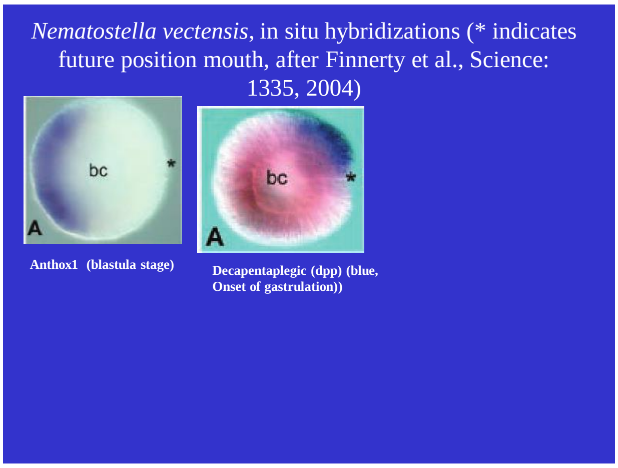

Nematostella vectensis, in situ hybridizations (* indicates future position mouth, after Finnerty et al., Science: 1335, 2004)

Anthox1 (blastula stage)

Decapentaplegic (dpp) (blue, Onset of gastrulation))

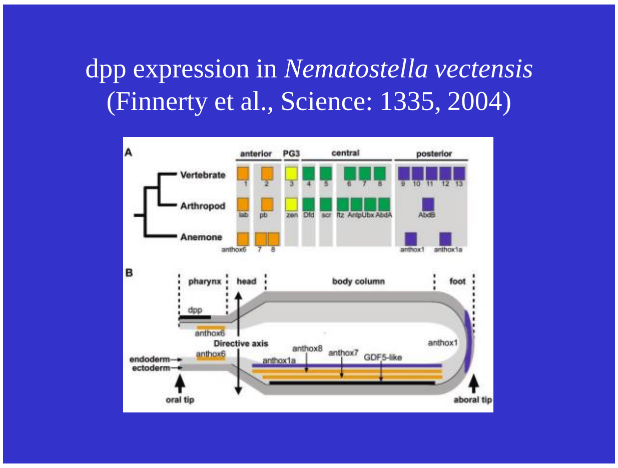

dpp expression in *Nematostella vectensis* (Finnerty et al., Science: 1335, 2004)

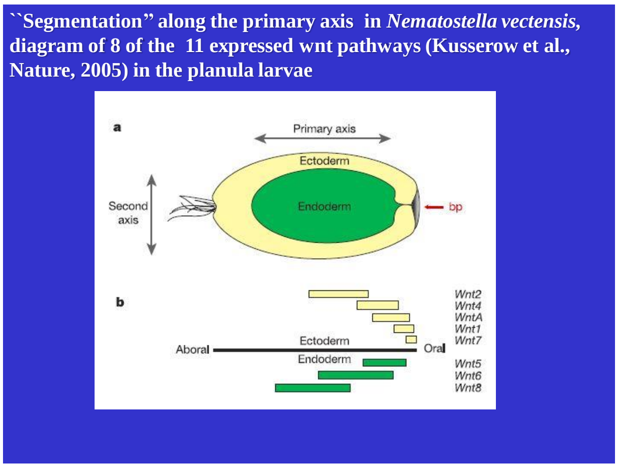

``Segmentation” along the primary axis in *Nematostella vectensis*, diagram of 8 of the 11 expressed wnt pathways (Kusserow et al., Nature, 2005) in the planula larvae

- Modelling and inferring gene regulatory networks in *Nematostella vectensis*, (Botman et al., Plos One, 2014; Abdol et al., Dev. Biol. 2017; Vroomans et al., in prep**)**

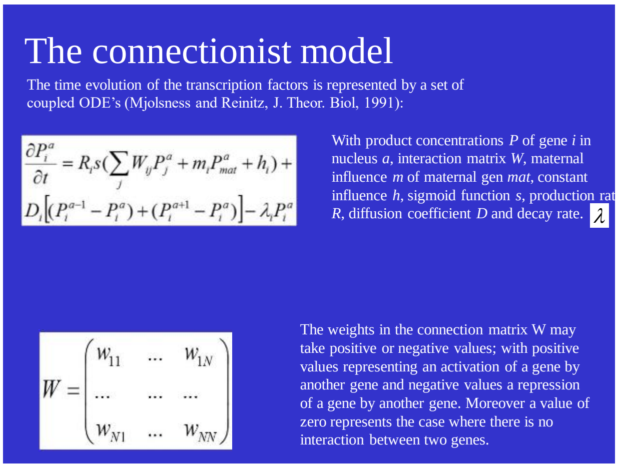

The connectionist model

The time evolution of the transcription factors is represented by a set of coupled ODE’s (Mjolsness and Reinitz, J. Theor. Biol, 1991):

$$\frac{\partial P_i^a}{\partial t} = R_i s(\sum_j W_{ij} P_j^a + m_i P_{mat}^a + h_i) + D_i\left[(P_i^{a-1} - P_i^a) + (P_i^{a+1} - P_i^a)\right] - \lambda_i P_i^a$$

With product concentrations *P* of gene *i* in nucleus *a*, interaction matrix *W*, maternal influence *m* of maternal gen *mat*, constant influence *h*, sigmoid function *s*, production rat *R*, diffusion coefficient *D* and decay rate. λ

$$W = \begin{pmatrix} w_{11} & \dots & w_{1N} \\ \dots & \dots & \dots \\ w_{N1} & \dots & w_{NN} \end{pmatrix}$$

The weights in the connection matrix W may take positive or negative values; with positive values representing an activation of a gene by another gene and negative values a repression of a gene by another gene. Moreover a value of zero represents the case where there is no interaction between two genes.

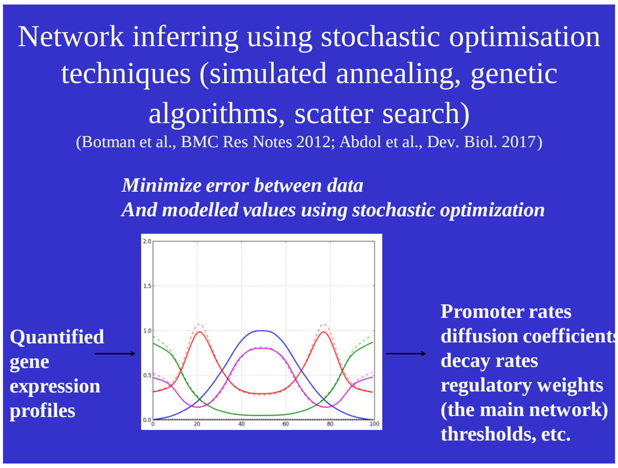

Network inferring using stochastic optimisation techniques (simulated annealing, genetic algorithms, scatter search)

(Botman et al., BMC Res Notes 2012; Abdol et al., Dev. Biol. 2017)

Minimize error between data
And modelled values using stochastic optimization

Quantified gene expression profiles →

→ **Promoter rates**
diffusion coefficients
decay rates
regulatory weights
(the main network)
thresholds, etc.

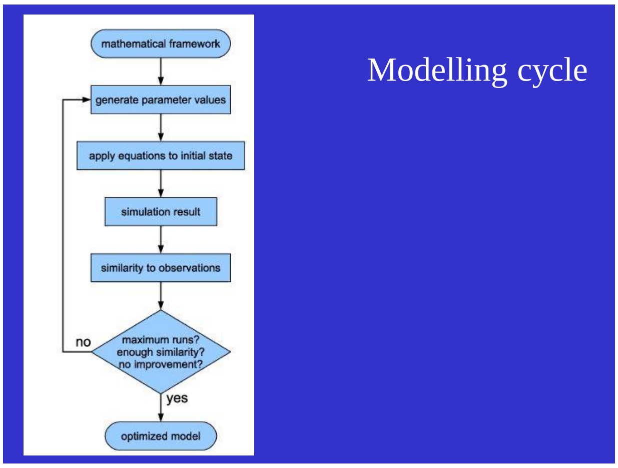

Modelling cycle

mathematical framework
generate parameter values
apply equations to initial state
simulation result
similarity to observations
maximum runs? enough similarity? no improvement?
no
yes
optimized model

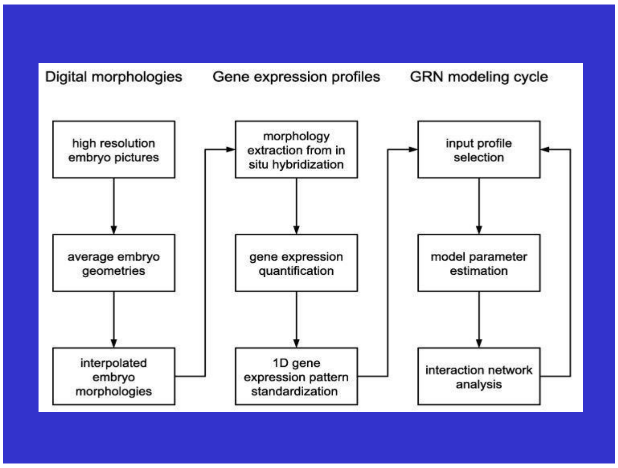

Digital morphologies
high resolution embryo pictures
average embryo geometries
interpolated embryo morphologies

Gene expression profiles
morphology extraction from in situ hybridization
gene expression quantification
1D gene expression pattern standardization

GRN modeling cycle
input profile selection
model parameter estimation
interaction network analysis

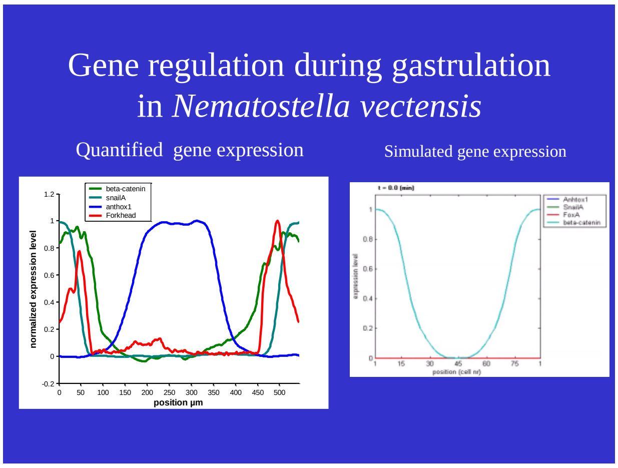

Gene regulation during gastrulation in *Nematostella vectensis*

Quantified gene expression

Simulated gene expression

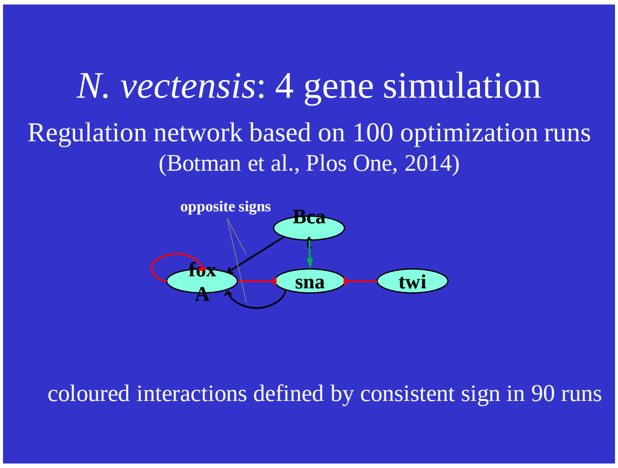

N. vectensis: 4 gene simulation

Regulation network based on 100 optimization runs
(Botman et al., Plos One, 2014)

coloured interactions defined by consistent sign in 90 runs

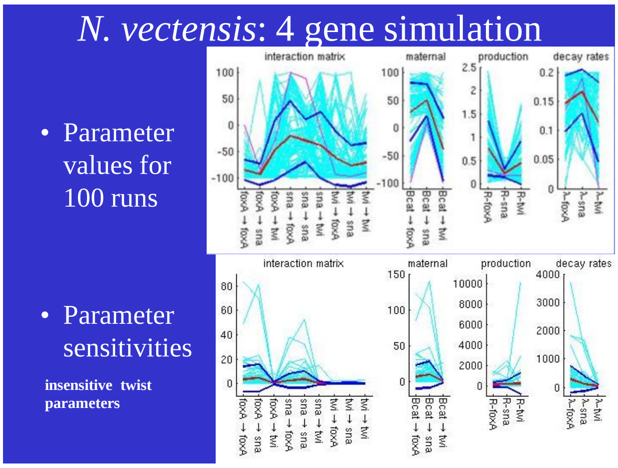

N. vectensis: 4 gene simulation

- Parameter values for 100 runs
- Parameter sensitivities

insensitive twist parameters

55

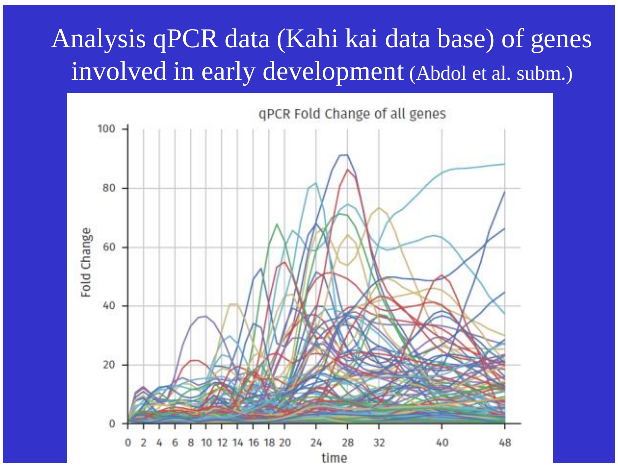

Analysis qPCR data (Kahi kai data base) of genes involved in early development (Abdol et al. subm.)

56

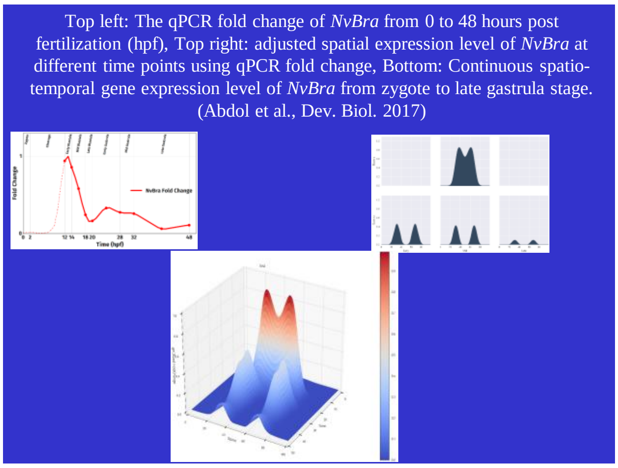

Top left: The qPCR fold change of *NvBra* from 0 to 48 hours post fertilization (hpf), Top right: adjusted spatial expression level of *NvBra* at different time points using qPCR fold change, Bottom: Continuous spatio-temporal gene expression level of *NvBra* from zygote to late gastrula stage. (Abdol et al., Dev. Biol. 2017)

57

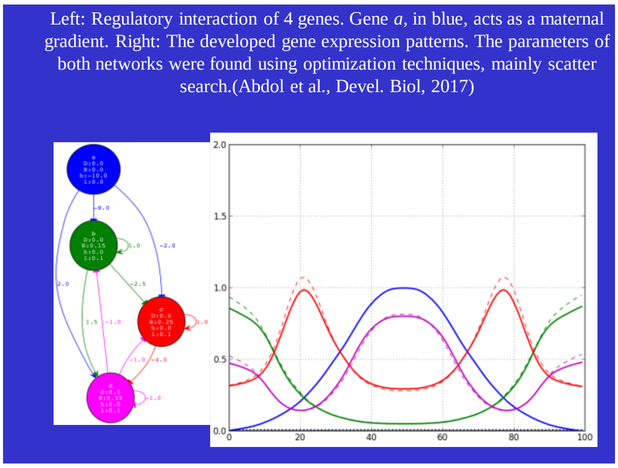

Left: Regulatory interaction of 4 genes. Gene *a*, in blue, acts as a maternal gradient. Right: The developed gene expression patterns. The parameters of both networks were found using optimization techniques, mainly scatter search.(Abdol et al., Devel. Biol, 2017)

58

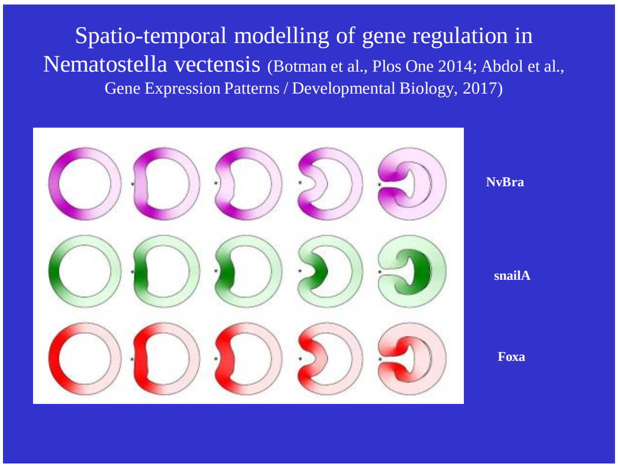

Spatio-temporal modelling of gene regulation in Nematostella vectensis (Botman et al., Plos One 2014; Abdol et al., Gene Expression Patterns / Developmental Biology, 2017)

59

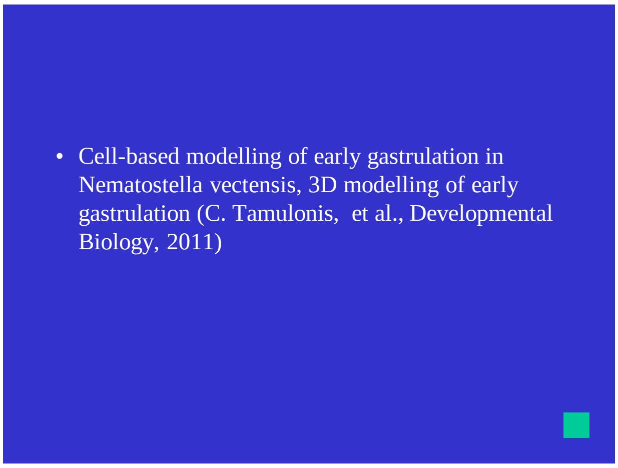

- Cell-based modelling of early gastrulation in Nematostella vectensis, 3D modelling of early gastrulation (C. Tamulonis, et al., Developmental Biology, 2011)

60

Nv gastrulation V

Invagination

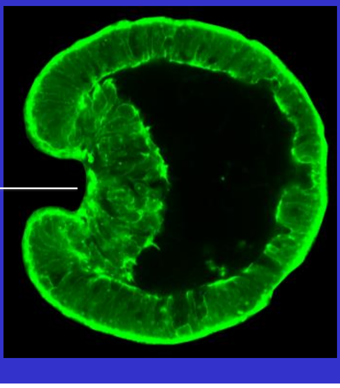

Apical constriction also induces invagination

Nematostella vectensis gastrulation modelling goals

- Better understand the role of the individual processes in the collective gastrulation process
- Understand gastrulation variability through parameter variation
- Understand why gastrulation in *Nematostella vectensis* is so robust despite high variability

Cell representation

- Cell boundary represented as a detailed polygon
- Polygon is defined as a sequence of points
- Differential properties across the boundary, e.g. apical region may be stiffer than the baso-lateral region

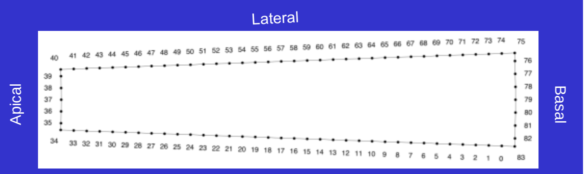

Physical cell model

- Each edge is loaded with a viscoelastic element
- Elastic element restrains the cell area
- The dynamics of the model are driven by simple Newtonian mechanics, running a simulation step consists of determining the forces acting on each vertex and the resulting system of differential equations is solved using the Velocity Verlet numerical integration method

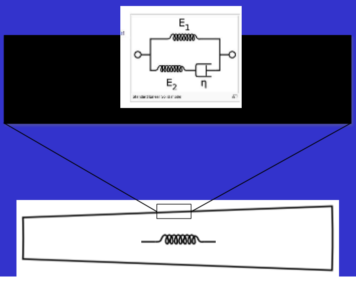

Cell-Based modelling: dynamics

- The dynamics of the model are driven by simple Newtonian mechanics and the position of each vertex, $\mathbf{r}_{c,i}$ is governed by the equation:

$$m_{c,i}\frac{d^2 r_{c,i}}{dt^2} = F_{c,i} - \eta_{c,i}\frac{dr_{c,i}}{dt} \qquad c = 1,\ldots,87 \qquad v = 1,\ldots,84$$

- Where $\mathbf{F}_{c,i}$ is the total force acting on the vertex, $m_{c,i}$ and $\eta_{c,i}$ are the mass and the damping parameter of the vertex.
- All the processes in the model are described in terms of vector forces. Running a simulation step consists of determining the forces acting on each vertex and solving the resulting system of differential equations is solved using the Velocity verlet numerical integration method with timestep .

Forces I: springs

- Each edge of every cell is loaded with a spring that controls its length by exerting a restorative force proportional to the strain

$$F = k\frac{l - l_0}{l_0}$$

- Where k is the spring stiffness, l is the edge length and l_0 is the spring's rest length

Forces II: Cytosol

- The area of a cell is given by the standard formula for the area of a polygon

$$-\frac{1}{2}\sum_{i=1}^{84} r_i \times r_{i+1} = -\frac{1}{2}\sum_{i=1}^{84} x_i y_{i+1} - x_{i+1} y_i$$

- The inner contents of a cell are assumed elastic with energy

$$E = \frac{1}{2} k_V \left(\frac{A - A_0}{A_0} \right)^2$$

- where *A* is the area of the cell, *A0* is the equilibrium area of the cell (equal to the initial area of the cell) and K_A is the stiffness of the inner area.

67

Forces III

- Contact forces are defined between edge-vertex pairs
- Filopodia: long range adhesive mechanism

68

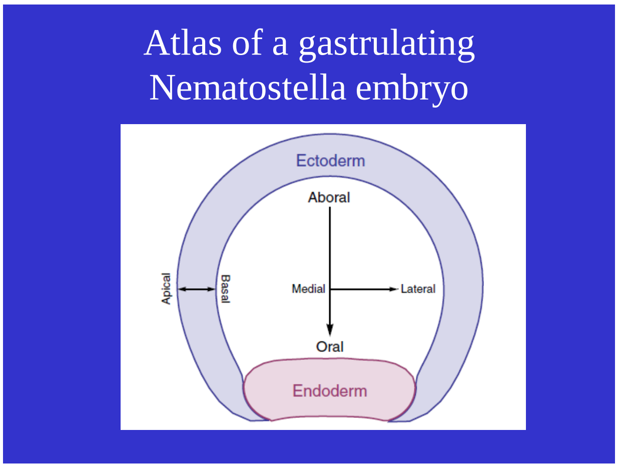

Atlas of a gastrulating Nematostella embryo

69

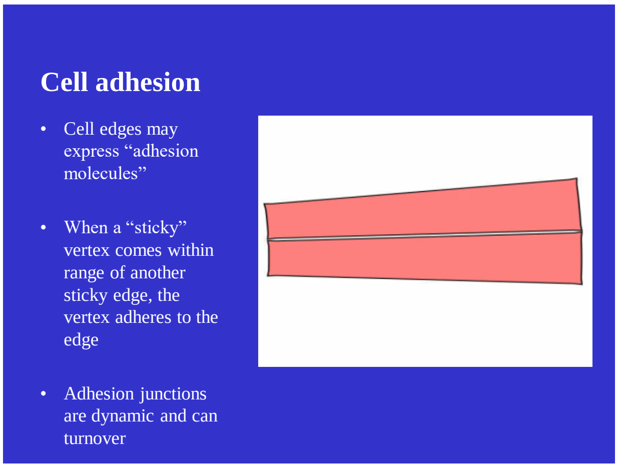

Cell adhesion

- Cell edges may express “adhesion molecules”
- When a “sticky” vertex comes within range of another sticky edge, the vertex adheres to the edge
- Adhesion junctions are dynamic and can turnover

70

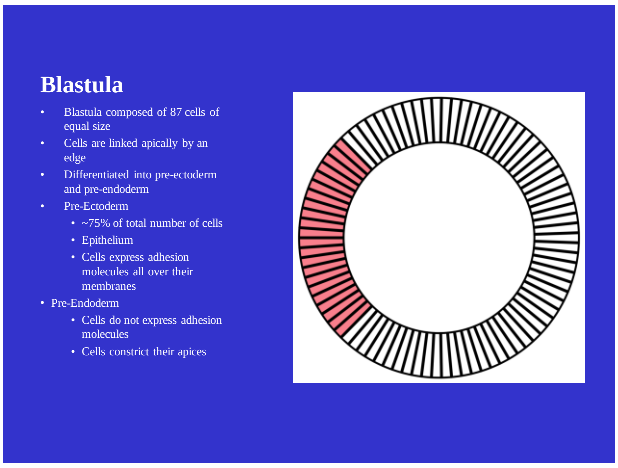

Blastula

- Blastula composed of 87 cells of equal size
- Cells are linked apically by an edge
- Differentiated into pre-ectoderm and pre-endoderm
- Pre-Ectoderm
  - ~75% of total number of cells
  - Epithelium
  - Cells express adhesion molecules all over their membranes
- Pre-Endoderm
  - Cells do not express adhesion molecules
  - Cells constrict their apices

71

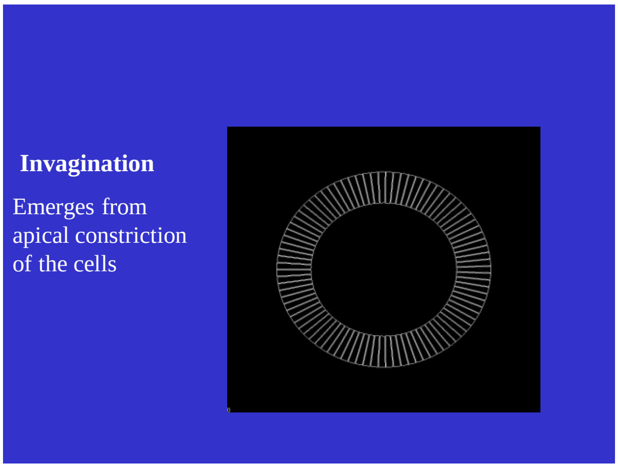

Invagination

Emerges from apical constriction of the cells

72

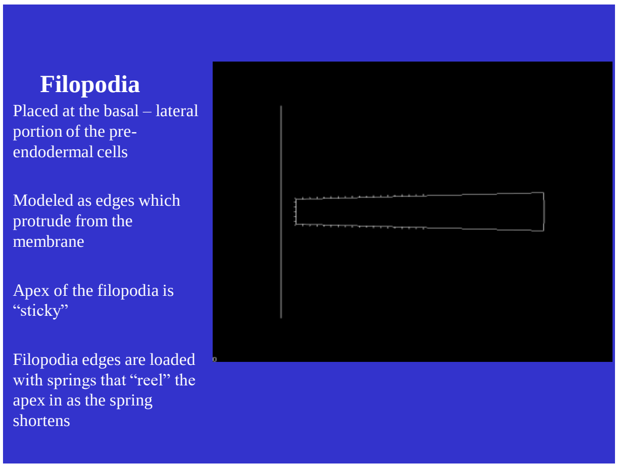

Filopodia

Placed at the basal – lateral portion of the pre-endodermal cells

Modeled as edges which protrude from the membrane

Apex of the filopodia is "sticky"

Filopodia edges are loaded with springs that "reel" the apex in as the spring shortens

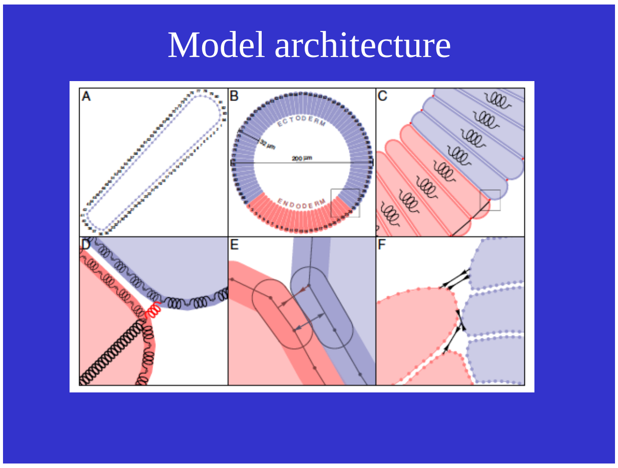

Model architecture

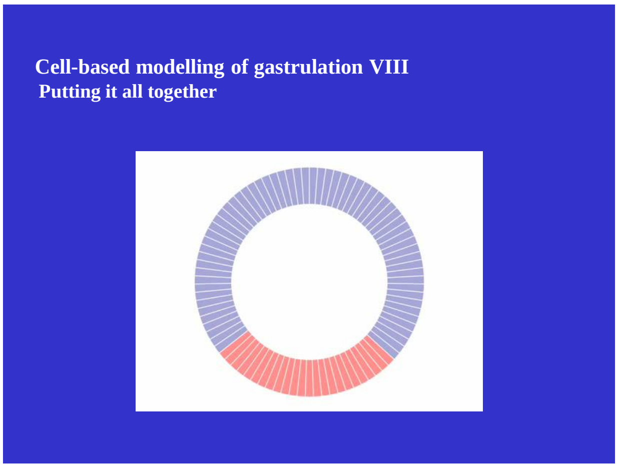

Cell-based modelling of gastrulation VIII

Putting it all together

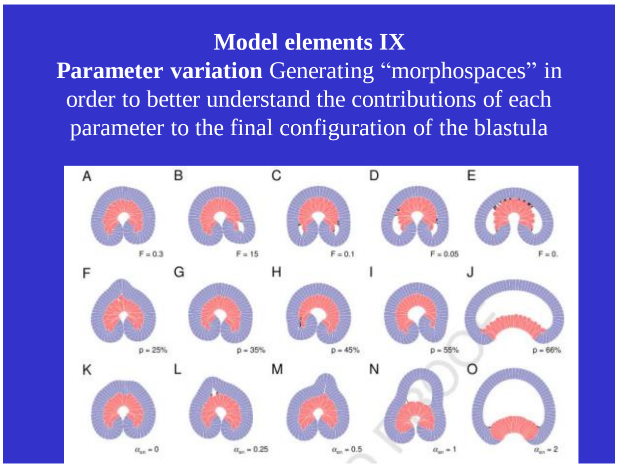

Model elements IX

Parameter variation Generating "morphospaces" in order to better understand the contributions of each parameter to the final configuration of the blastula

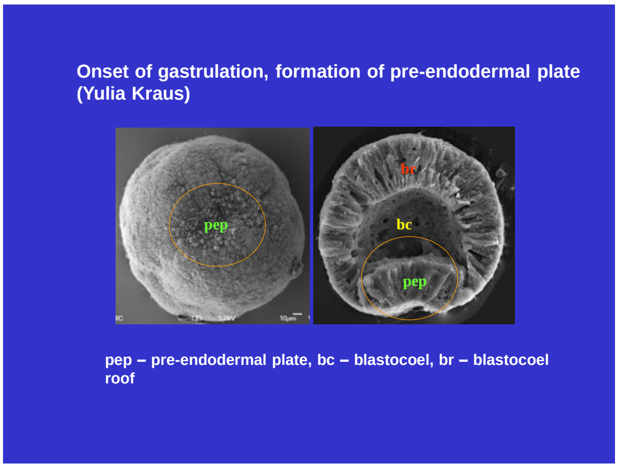

Onset of gastrulation, formation of pre-endodermal plate (Yulia Kraus)

pep – pre-endodermal plate, bc – blastocoel, br – blastocoel roof

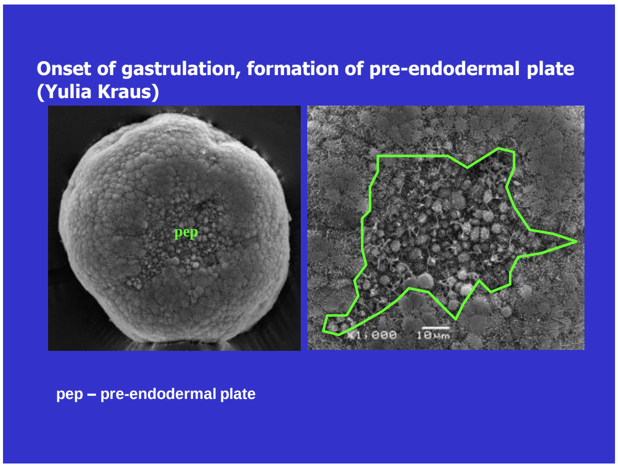

Onset of gastrulation, formation of pre-endodermal plate (Yulia Kraus)

pep – pre-endodermal plate

3D cell based modelling of gastrulation, preliminary example (R.dries, F. Jansson and J.A. Kaandorp, in prep.)

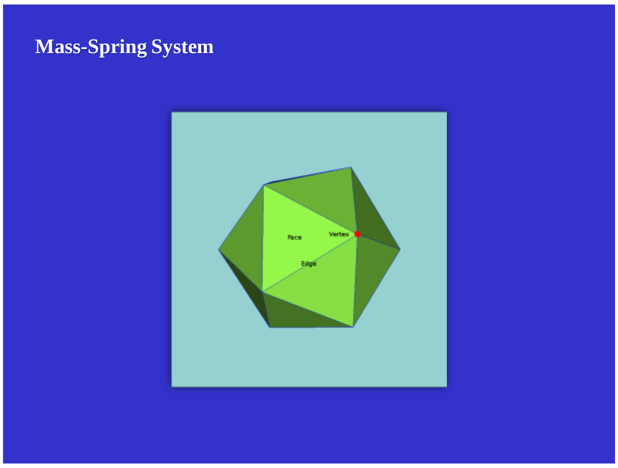

Mass-Spring System

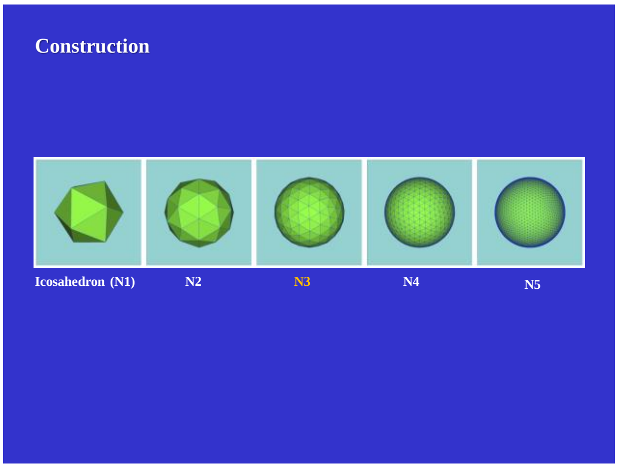

Construction

Icosahedron (N1) N2 N3 N4 N5

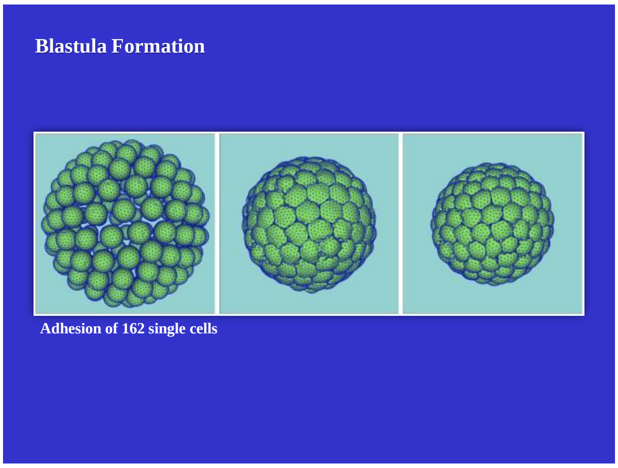

Blastula Formation

Adhesion of 162 single cells

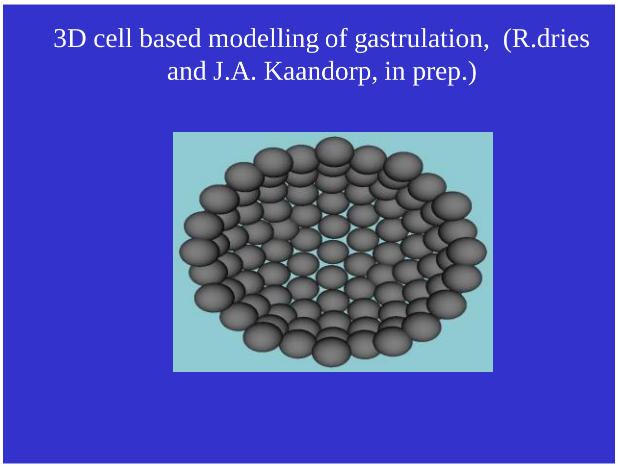

3D cell based modelling of gastrulation, (R.dries and J.A. Kaandorp, in prep.)

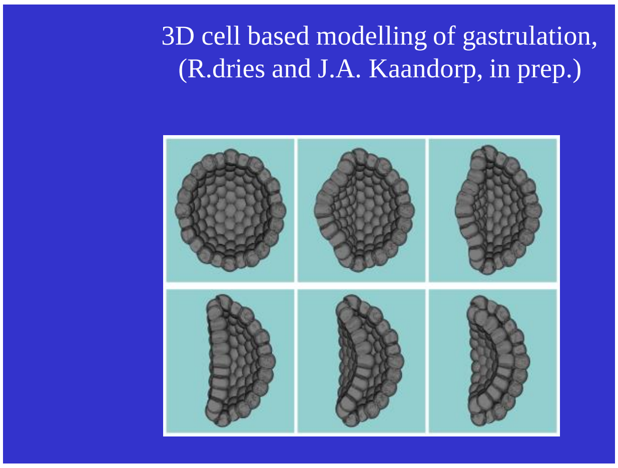

3D cell based modelling of gastrulation, (R.dries and J.A. Kaandorp, in prep.)

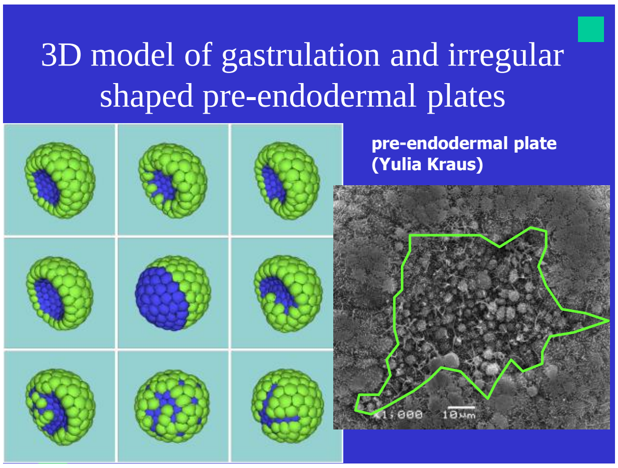

3D model of gastrulation and irregular shaped pre-endodermal plates

pre-endodermal plate (Yulia Kraus)

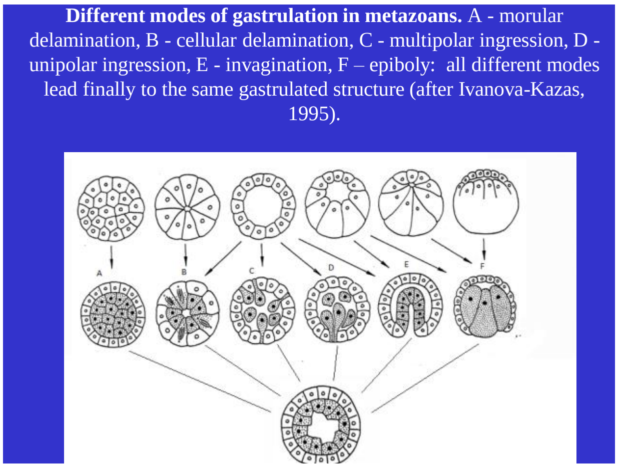

Different modes of gastrulation in metazoans. A - morular delamination, B - cellular delamination, C - multipolar ingression, D - unipolar ingression, E - invagination, F – epiboly: all different modes lead finally to the same gastrulated structure (after Ivanova-Kazas, 1995).

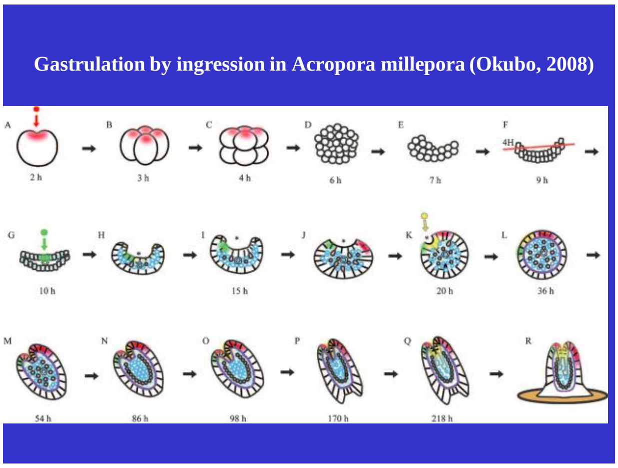

Gastrulation by ingression in Acropora millepora (Okubo, 2008)

Gastrulation in the hydrozoan *Clytia hemisphaerica*

- Gastrulation by ingressiion

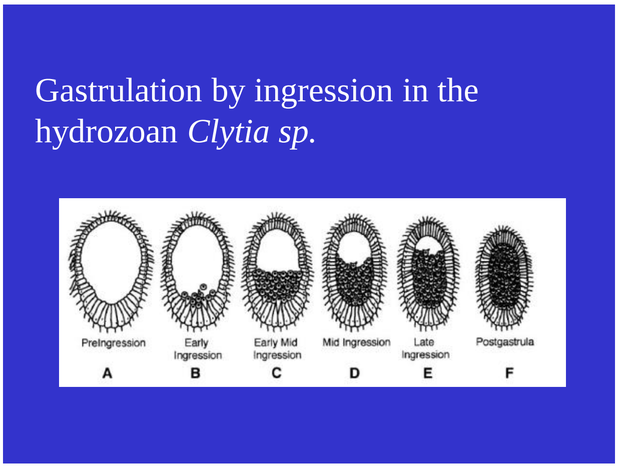

Gastrulation by ingression in the hydrozoan *Clytia sp.*

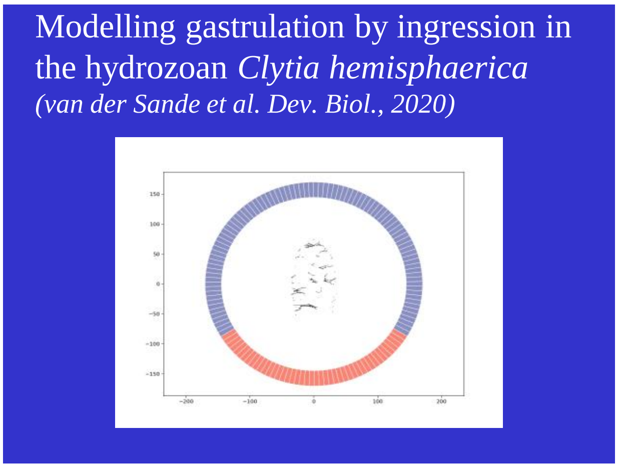

Modelling gastrulation by ingression in the hydrozoan *Clytia hemisphaerica*

(van der Sande et al. Dev. Biol., 2020)

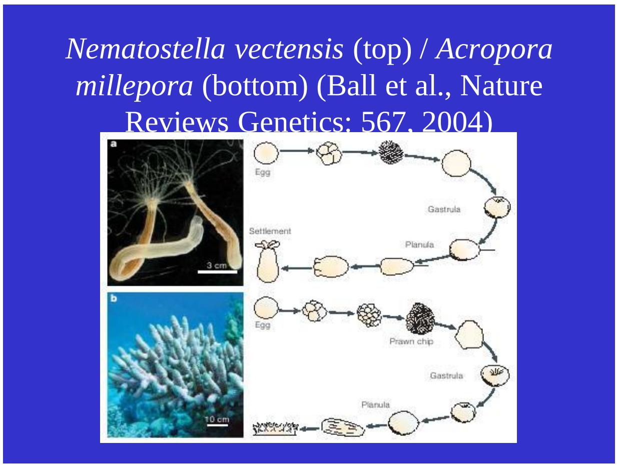

Nematostella vectensis (top) / *Acropora millepora* (bottom) (Ball et al., Nature Reviews Genetics: 567, 2004)

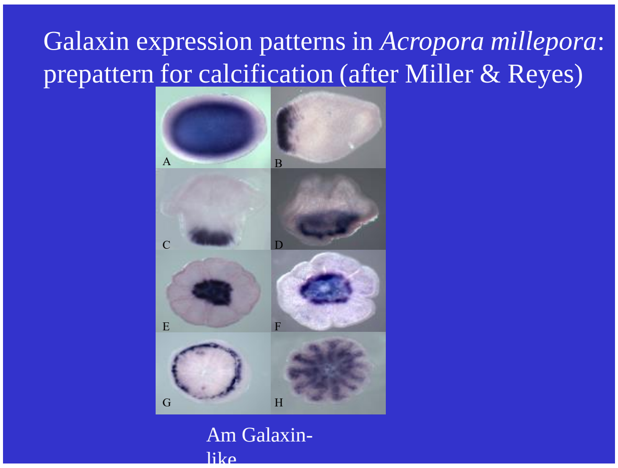

Galaxin expression patterns in *Acropora millepora*: prepattern for calcification (after Miller & Reyes)

Am Galaxin-like

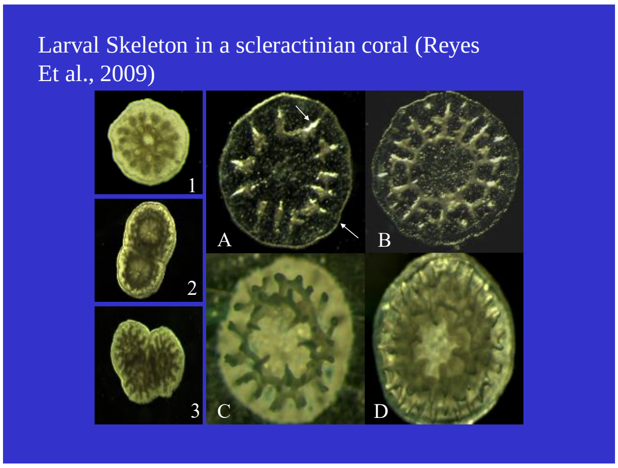

Larval Skeleton in a scleractinian coral (Reyes Et al., 2009)

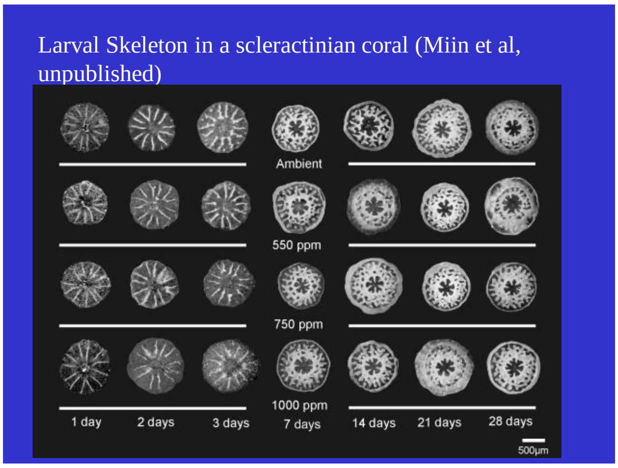

Larval Skeleton in a scleractinian coral (Miin et al, unpublished)

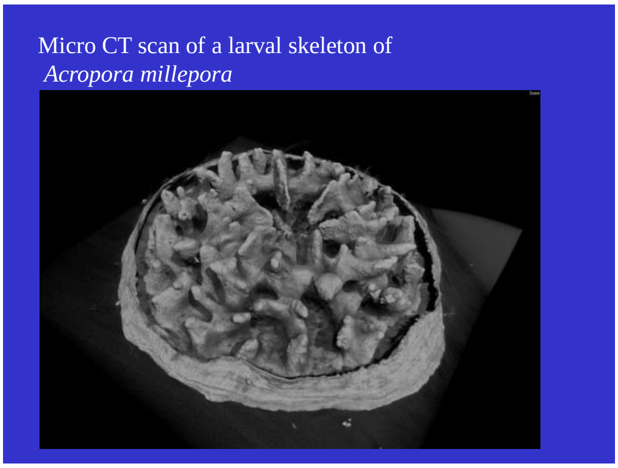

Micro CT scan of a larval skeleton of *Acropora millepora*

Conclusions and future work

- Robust 2D model gastrulation, we can demonstrate bottle cell formation, apical constriction and gastrulation
- Couple the gastrulation model with a model of gene regulation
- Extend this model to other species (e.g. *Acropora millepora*, other types of gastrulation, e.g. species with ingression)
- Develop a 3D model of gastrulation and gene regulation

Multi-scale modelling of calcification in cnidarians II

Jaap A. Kaandorp
Computational Science Lab
Faculty of Science
University of Amsterdam
Science Park 904, 1098 XH Amsterdam
The Netherlands
E-mail: J.A.Kaandorp@uva.nl
http://www.science.uva.nl/~jaapk

Overview

- Modelling gene regulation
- The sea anemone *Nematostella vectensis* case study modelling gene regulation
- Cell-based modelling of gastrulation in *Nematostella* and the hydrozoan *Clytia hemisphaerica*
- Biomineralisation in the scleractinian coral *Acropora millepora*
- Modelling calcification physiology in corals
- Modelling growth and form of corals (e.g *Madracis sp.*) and the impact of the physical environment

Nematostella vectensis (top) / *Acropora millepora* (bottom) (Ball et al., Nature Reviews Genetics: 567, 2004)

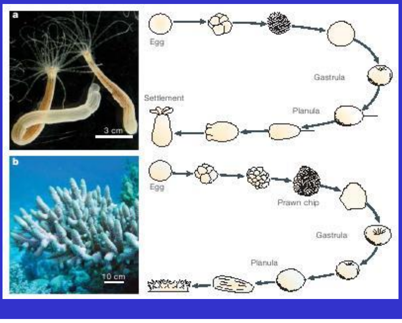

Growth of corals: a multiscale problem

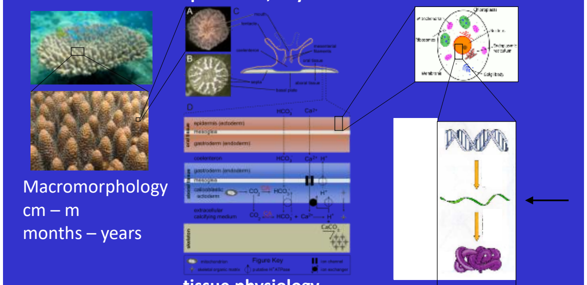

Micromorphology
µm – mm; days - weeks

cell physiology
1 – 10 µm; ns - hours

Macromorphology
cm – m
months – years

tissue physiology
1 – 100 µm; ns -µs

molecular physiology
Å – nm; s - mins

Great Barrier Reef Australia I

Great Barrier Reef Australia II

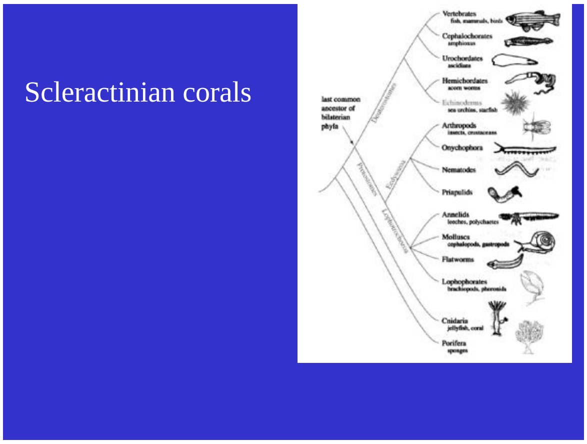

Scleractinian corals

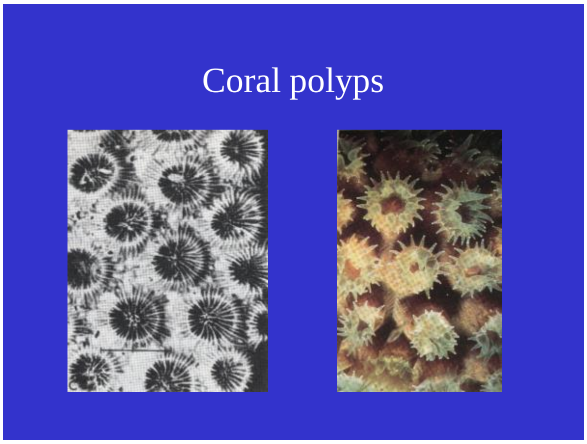

Coral polyps

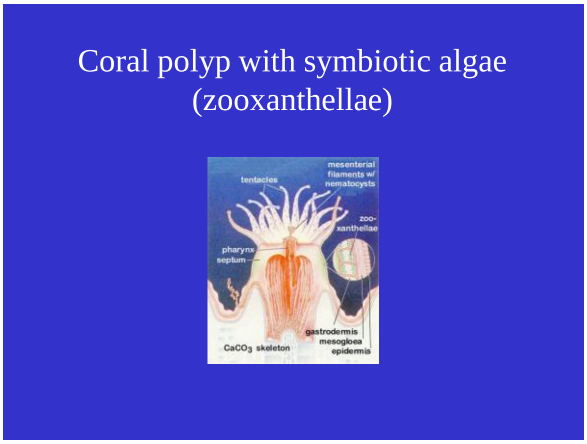

Coral polyp with symbiotic algae (zooxanthellae)

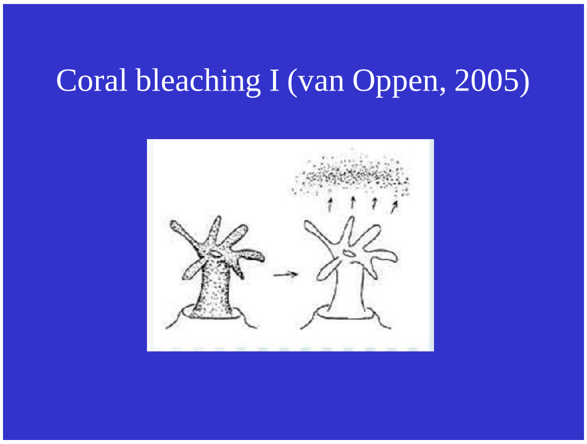

Coral bleaching I (van Oppen, 2005)

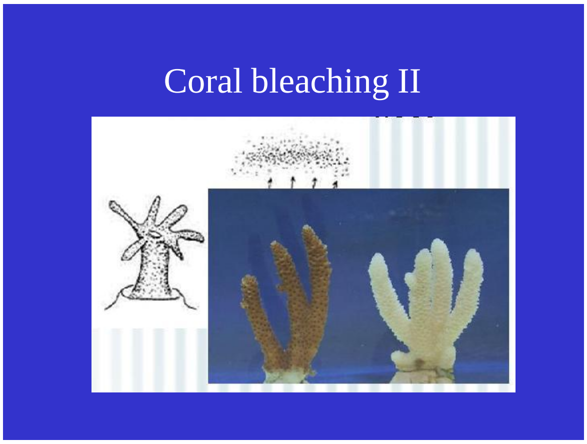

Coral bleaching II

Coral bleaching III

Calcification and CO_2

photosynthesis

$$CO_2 + H_2O \rightarrow CH_2O + O_2 \qquad (1)$$

respiration

$$CH_2O + O_2 \rightarrow CO_2 + H_2O \qquad (2)$$

calcification

$$Ca^{2+} + 2HCO_3^- \rightarrow CaCO_3 + CO_2 + H_2O \qquad (3)$$

equilibrium reaction

$$CO_2 + H_2O \leftrightarrows H^+ + HCO_3^- \qquad (4)$$

Acidification of oceans I

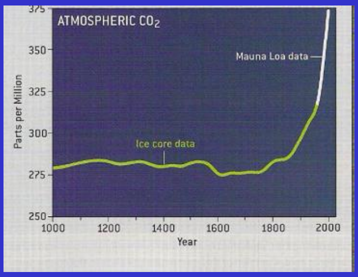

(Veron, 2009)

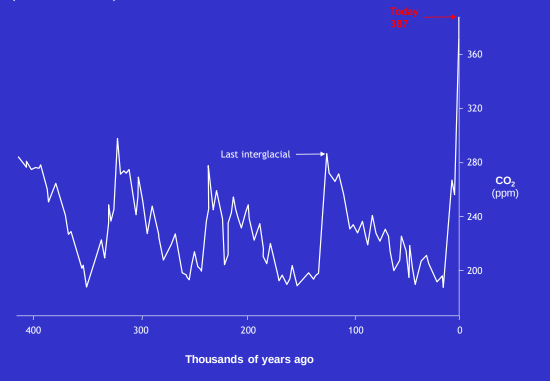

(Veron, 2009)

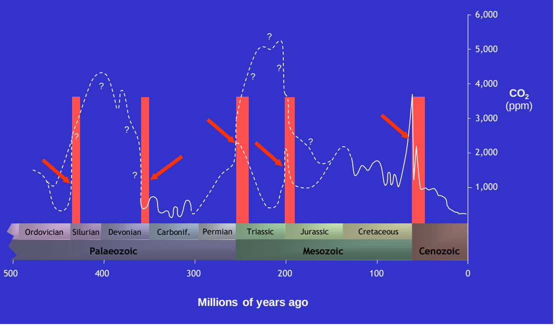

Changes in carbonate chemistry in surface seawater (Gattuso, 2008)

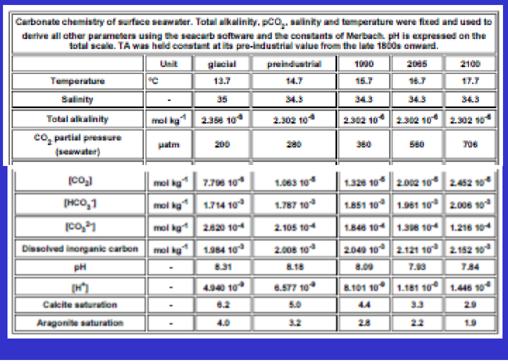

Carbonate chemistry of surface seawater. Total alkalinity, pCO_2, salinity and temperature were fixed and used to derive all other parameters using the seacarb software and the constants of Merbach. pH is expressed on the total scale. TA was held constant at its pre-industrial value from the late 1800s onward.

	Unit	glacial	preindustrial	1990	2065	2100
Temperature	°C	13.7	14.7	15.7	16.7	17.7
Salinity	-	35	34.3	34.3	34.3	34.3
Total alkalinity	mol kg^{-1}	$2.356\ 10^{-3}$	$2.302\ 10^{-3}$	$2.302\ 10^{-3}$	$2.302\ 10^{-3}$	$2.302\ 10^{-3}$
CO_2 partial pressure (seawater)	µatm	200	280	380	560	706
$[CO_2]$	mol kg^{-1}	$7.796\ 10^{-6}$	$1.063\ 10^{-5}$	$1.326\ 10^{-5}$	$2.002\ 10^{-5}$	$2.452\ 10^{-5}$
$[HCO_3^-]$	mol kg^{-1}	$1.714\ 10^{-3}$	$1.787\ 10^{-3}$	$1.851\ 10^{-3}$	$1.961\ 10^{-3}$	$2.006\ 10^{-3}$
$[CO_3^{2-}]$	mol kg^{-1}	$2.620\ 10^{-4}$	$2.105\ 10^{-4}$	$1.846\ 10^{-4}$	$1.398\ 10^{-4}$	$1.216\ 10^{-4}$
Dissolved inorganic carbon	mol kg^{-1}	$1.984\ 10^{-3}$	$2.008\ 10^{-3}$	$2.049\ 10^{-3}$	$2.121\ 10^{-3}$	$2.152\ 10^{-3}$
pH	-	8.31	8.18	8.09	7.93	7.84
$[H^+]$	-	$4.940\ 10^{-9}$	$6.577\ 10^{-9}$	$8.101\ 10^{-9}$	$1.181\ 10^{-8}$	$1.446\ 10^{-8}$
Calcite saturation	-	6.2	5.0	4.4	3.3	2.9
Aragonite saturation	-	4.0	3.2	2.8	2.2	1.9

In summary

- Dissolving CO_2 in seawater increases the hydrogen ion ion (H+) concentration in the ocean and decreases ocean pH. Since the industrial revolution began, it is estimated that surface ocean pH has dropped by slightly less than 0.1 units (on the logarithmic scale of pH; approximately a 25% increase in H+), and it is estimated that it will drop by a further 0.3 to 0.5 units by 2100 as the oceans absorb more anthropogenic CO_2 (see also wikipedia, ocean acidification) "

$$CO_2 + CO_3^{-2} + H_2O \rightarrow 2HCO_3^-$$

- Dissolving CO_2 decreases carbonate ion(CO_3^{2-}) concentration in the ocean and lowers the saturation state of carbonate minerals (see also wikipedia, ocean acidification)

Saturation state of aragonite in corals (wikipedia)

- "The saturation state of seawater for a mineral(Ω) is a measure of the thermodynamic potential for the mineral to form or to dissolve; specifically it is the product of the concentrations (or activities) of the reacting ions that form the mineral (Ca^{2+} and CO_3^{2-}), divided by the product of the concentrations of those ions when the mineral is at equilibrium (K_{sp}), that is, when the mineral is neither forming nor dissolving.

$$\Omega_{sp} = \frac{[Ca^{2+}][CO_3^{-2}]}{K_{sp}}$$

- In seawater, a natural boundary is formed as a result of temperature, pressure, and depth, and is known as the saturation horizon. It is above this saturation horizon that calcifying organisms live, as CaCO3 does not readily dissolve there
- Calcium carbonate exists in 2 commonly occurring forms: aragonite and calcite. The aragonite form is much more soluble than the calcite form which means that the aragonite saturation horizon is always nearer to the surface than the calcite saturation horizon. This means that those organisms that produce calcite may possibly be less vulnerable to changes in ocean acidity than those which produce aragonite (the scleractinian corals).

$CaC0_3$ Crystals

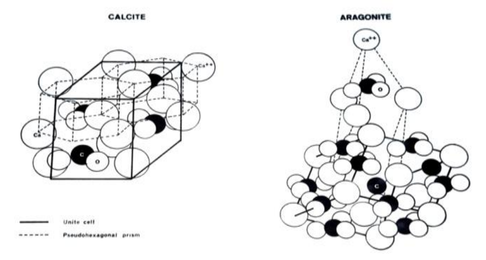

carbonate minerals

Aragonite

Calcite

Aragonite saturation state vs calcification rate (Leclerq et al., 2000)

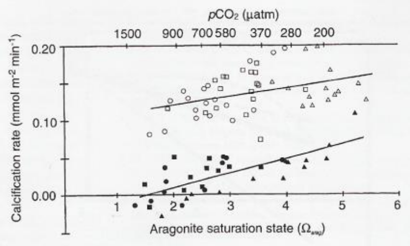

What do *Acropora* skeletal proteins tell us about coral biocalcification ?

Ramos-Silva, F. Marin, J.A. Kaandorp, and B. Marie, PNAS, 3–5. 2013

- P. Ramos-Silva J.A, Kaandorp, L. Huisman, B. Marie, I. Zanella-Cléon4, N. Guichard, D.J. Miller and F. Marin, Molecular Biology and Evolution, 2013

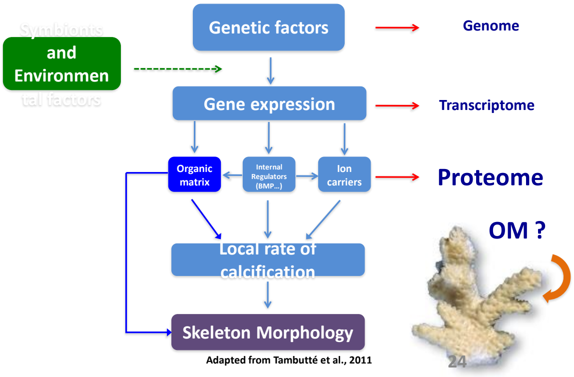

Adapted from Tambutté et al., 2011

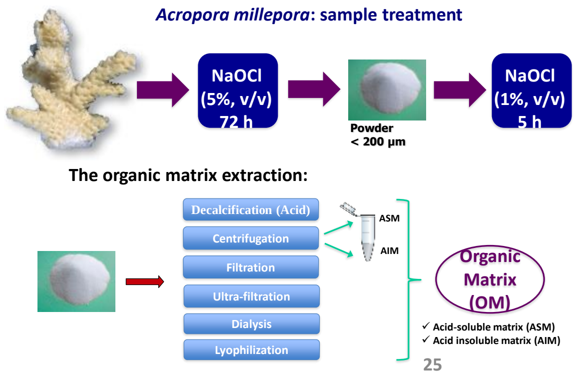

Acropora millepora: sample treatment

NaOCl (5%, v/v) 72 h

Powder
< 200 µm

NaOCl (1%, v/v) 5 h

The organic matrix extraction:

- Decalcification (Acid)
- Centrifugation
- Filtration
- Ultra-filtration
- Dialysis
- Lyophilization

ASM

AIM

Organic Matrix (OM)

✓ Acid-soluble matrix (ASM)
✓ Acid insoluble matrix (AIM)

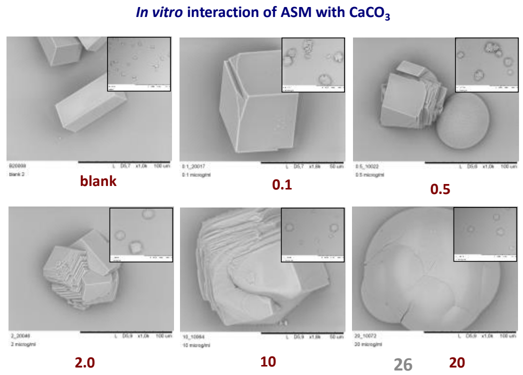

In vitro interaction of ASM with $CaCO_3$

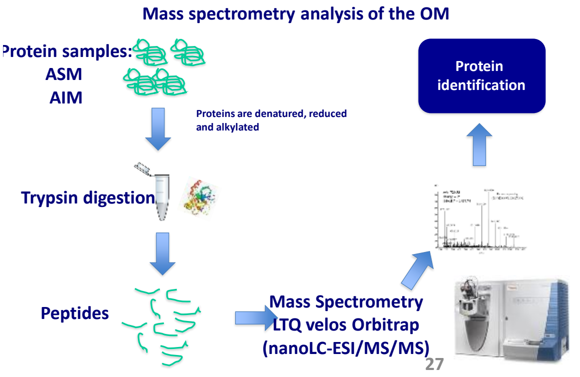

Mass spectrometry analysis of the OM

Protein samples:
ASM
AIM

Proteins are denatured, reduced and alkylated

Trypsin digestion

Peptides

Mass Spectrometry
LTQ velos Orbitrap
(nanoLC-ESI/MS/MS)

Protein identification

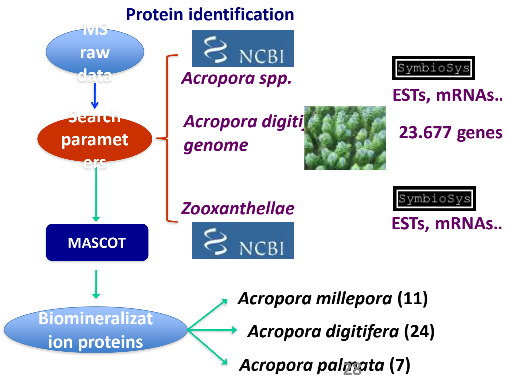

Protein identification

MS raw data

Search parameters

MASCOT

Biomineralization proteins

Acropora spp.

Acropora digiti *genome*

Zooxanthellae

ESTs, mRNAs..

23.677 genes

ESTs, mRNAs..

Acropora millepora (11)
Acropora digitifera (24)
Acropora palmata (7)

Protein analysis

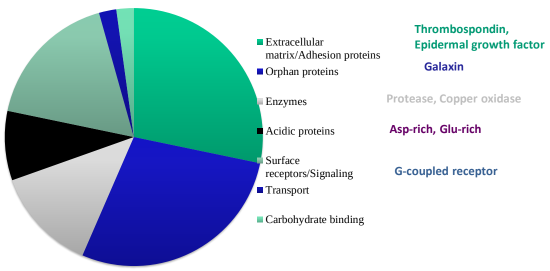

Distribution of functions from proteins of the ASM

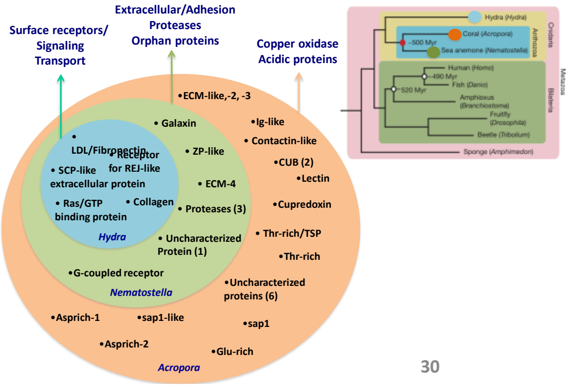

Conclusions

- First attempt to fully characterize the organic matrix of a reef coral using proteomics together with the available genomic resources
- Confirmed the presence of highly acidic proteins, unknown domains and known domains also reported on other OM such as mollusks (ex: von Willebrand factor domain)
- 3 proteins with homology in other Cnidaria than Corals.

Towards a quantitative spatio-temporal model of calcification physiology in a scleractinian coral *(submitted)*

Helena Willard, Eva Deutekom, Denis Allemand & Jaap Kaandorp
Computational Science Lab
University of Amsterdam

Scale levels focused on

Tissue physiology

Gene transcription
Protein production
Regulation

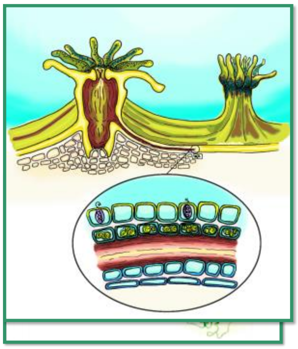

Calcification in reef building corals

- Consensus that **enhanced calcifying medium (ECM)** is chemically controlled by calicoblastic cells *to enhance calcification.*
- What does calcification need?
  - Calcium ions (Ca^{2+})
  - Carbonate ions (CO_3^{2-})
    - Dissolved inorganic carbon (DIC)
    - High pH to deprotonate DIC

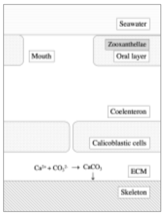

Existing hypotheses

- **1. Diffusion of CO_2**
- **2. Paracellular transport**
- **3. Transcellular transport using ion-transporters** [1 2 3 4 5]
- **4. HCO_3^- Transporter** [5 6]
- **5. Respiration** [5]
- **6. Carbonic Anhydrase** [1 7 8]
- **7. Vesicles** [9]

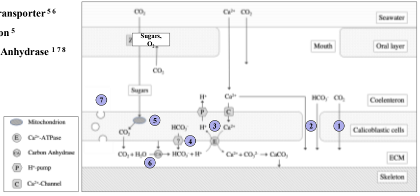

Light Enhanced Calcification

- **Calcification rate is known to increase in light conditions** [1 2 4]
- **1. Photosynthesis in zooxanthellae**
  - **1a. More DIC available due to increased metabolism** [1 3]
  - **1b. More energy available in Calicoblastic cells for active transport and excreting OM** [1 2 3]
- **2. Ca^{2+}-ATPase light sensitive** [2]

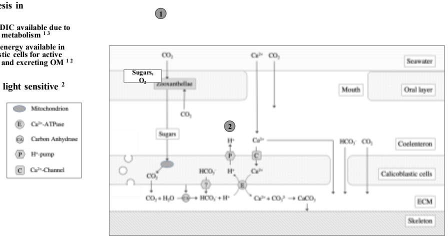

Existing Models

- Reaction-Diffusion model of Yuan (2018) [10]
  - (+) Detailed analysis of CO_2-chemistry by modelling chemical system
  - (+) Includes diffusion and spatial processes such as photosynthesis and calcification
  - (-) *No information on chemical composition in ECM*
  - (-) *No temporal information*

Existing Models

- Compartmental model of Nakamura (2013) [3]
  - (+) Detailed analysis of chemical composition in ECM
  - (+) Able to model LEC
  - (+) Has some nice energy calculations, incl. photosynthesis and respiration
  - (-) Does *not include diffusion of chemical compounds*
  - (-) Does not model the chemical reactions of the carbonate acid-base system but *assumes the system to be in equilibrium.*
    - Uses one of the CO_2-chemistry packages

Calculating carbonate-chemistry

- Some articles calculate chemical composition of the ECM using a CO_2-system, assuming that the system is in equilibrium. [10 11]
  - *Or steady-state, meaning the concentrations are constant*
  - Including the article of Raybaud (2017) [11]
- Many mathematical models available to make these calculations, including CO2sys, csys [12]
  - These packages might not be suitable for calculations like these because they assume a closed environment, where no chemicals are going in or out.
  - While in the *ECM is not a closed system*
    - Chemicals go out (calcification, removal of protons) and go in (ion-transport, CO_2 diffusion)

Closed model

- In our computations we use the mathematical model for the CO_2-chemistry as proposed by Zeebe (2001) and solve them in COMSOL
- The chemical composition of the system follows from two parameters
  - 1. Dissolved Inorganic Carbon (DIC)
    - DIC = CO2 + HCO3 + CO3
  - 2. Total Alkalinity (TA)
    - Sum of conjugated bases, describes buffering capacity
    - TA = OH + HCO3 + 2*CO3 + BOH4 – H

Why modelling?

1. Testing four hypotheses about the transport of chemical agents in the calcifying tissue in a scleractinian coral

2. Testing four hypotheses on light enhanced calcification in an coral.

Closed model

- For every TA and DIC we obtain the steady-state values for pH and the saturation state Ω, indicated as pH* and Ω*
  - Domain DIC > TA not biologically relevant for the ECM

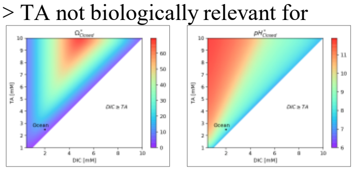

Based on figure in Raybaud (2017)[11]

Open model

- In this open model contains an ingoing fluxes (J_{CO2}) and two outgoing fluxes (J_H and J_{calc}), similar to ECM
- Keeping DIC and TA constant, we assume $J_{CO2} = J_H = J_{calc}$

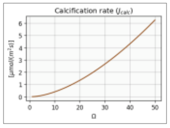

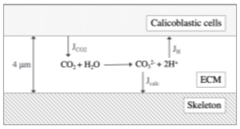

Open model

- For every set of DIC and TA we find a steady-state
- Steady-state values differ from closed system in some domains

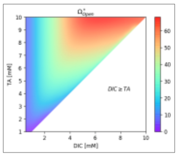

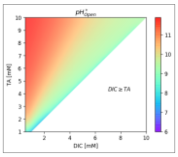

Comparing closed and open models

- Differences in steady-state values are quite significant in some domains, meaning that a close model might not always be suitable for calculating the chemical composition in the ECM.
- It is important to include the CO_2-chemistry reactions when modelling ECM.

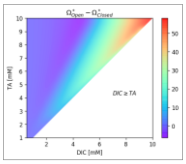

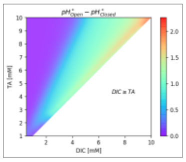

Our modelling approach

- Spatial model considering chemical processes controlling the chemical composition of the ECM.
- Both diffusion (spatial information) and chemical reactions.
- *Can we create a simple spatial model that reproduces data from in vivo measured data (e. g. Al Horani 2003) of the ECM in reef building corals?*
- *Can we, using this model, gain a better understanding on how the coral keeps the ECM's chemical composition favorable for calcification?*
- *Can we, using this model, reproduce the light-dark dynamics that are the effect of LEC?*

Our modelling approach

- Spatial Reaction-Diffusion model
  - Including CO_2-chemistry based on the system of Zeebe (2001)
- Simple topology
  - Cell membranes only permeable by CO_2
  - Calcification at skeleton boundary
  - Seawater constant concentrations

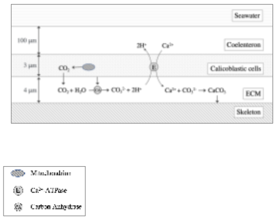

Our modelling approach

- Chemical composition ECM is controlled by
  - Respiration in Calicoblastic cells [5]
  - Ion transport of Ca^{2+}-ATPase [1 2 3 4 5]
    - Modelled as flux over Calicoblastic cells
    - $J_{ex} = J_{ex}^{max} \frac{[H^+]^2[Ca^{2+}]_{cell}}{K_{ex} + [H^+]^2[Ca^{2+}]_{cell}}$
  - Carbonic Anhydrase [1 7 8]
    - $V_{CA} = E(CA)_{tot}\, k_{cat} \frac{[CO_2]}{K_{CA} + [CO_2]}$

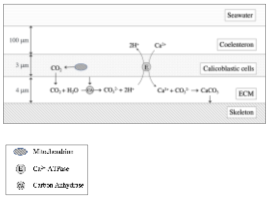

Our modelling approach

- System reaches steady state
  - – Flux of Ca^{2+}-ATPase equals calcification rate
  - – CO_2 – diffusion equals calcification rate

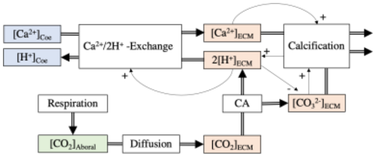

Our modelling approach

- We assume that, for every biologically relevant set of parameters, there exists at least one *stable* equilibrium point for which the concentrations in the ECM are constant. The latter also for biologically relevant ranges.
- The *chemical concentrations* corresponding to this equilibrium point are assumed to be controlled by the Calicoblastic cells.
- By understanding how this stable point is controlled, we might be able to simulate *the light-dark dynamics* as observed by, among others, Al-Horani (2003).

Steady State of the Model

- System shows one stable point
  - – {DIC*, TA*} = {3.1 mM, 4.6 mM}
    - These values correspond with literature [10 14]
  - – $\Omega^* = 24.1$
- Stable points seems global
  - – not formally proven
- Steady state is analyzed by changing
  - – J_{ex}^{max}
  - – R_{resp}
  - – $E(CA)_{tot}$

$E(CA)_{tot} = 0.05\mu mol$
$J_{max}^{ex} = 10\mu mol/(m^2 s)$
$R_{resp} = 2mM/s$

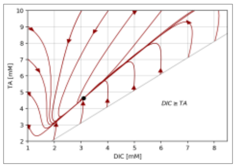

Changing J_{ex}^{max}

- High values for DIC* and TA* below a certain threshold, causing Ω* to decrease. These steady-states are not biologically relevant.
- Increasing J_{ex}^{max} does increase pH, but barely influences Ω*

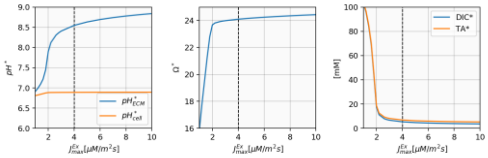

Changing R_{resp}

- Ω* seems to be controlled by the respiration rate
- Increasing respiration rate increases both DIC* and TA*
- Increasing respiration decreases pH*

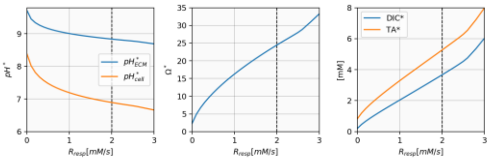

Changing $E(CA)_{tot}$

- Carbonic Anhydrase seems to play an important role in capturing DIC in the ECM, also controlling Ω*
- CA acidifies the ECM

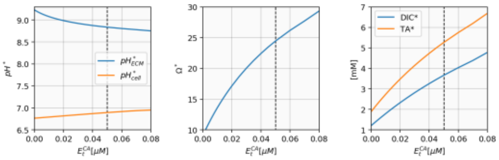

Conclusions

- Ω^* is barely dependent on the flux of Ca^{2+}-ATPase
- pH* is dependent on the flux of Ca^{2+}-ATPase
- When the flux of Ca^{2+}-ATPase is below a certain threshold, our steady states become biologically irrelevant
  - This threshold is probably correlated to the DIC supply
- Ω^* is strongly dependent on both R_{resp} and $E(CA)_{tot}$
- pH* increases as R_{resp} and $E(CA)_{tot}$ increase

Testing other hypotheses

- Paracellular transport
  - Paracellular space is assumed to be up to 20 nm

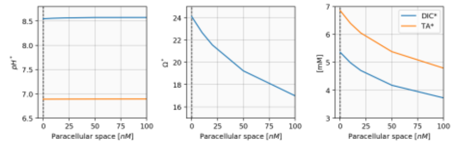

Testing other hypotheses

- Influence Ocean Acidification
  - Early results show that OA does not have a significant influence on Ω^*, but causes an increase of DIC* and TA*
  - Further research is needed to conclude this!

Light Enhanced Calcification

- Hypothesis 1: More DIC available due to increased metabolism [1 3]
- Hypothesis 2: Ca^{2+}-ATPase light sensitive [2]
- Hypothesis 3: Concentration CA is higher in dark conditions [7]

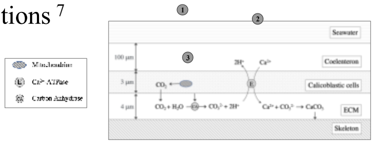

Light Enhanced Calcification

- Hypothesis 1: More DIC available due to increased metabolism [1 3]
- Hypothesis 2: Ca^{2+}-ATPase light sensitive [2]
- Hypothesis 3: Concentration CA is higher in dark conditions [7]

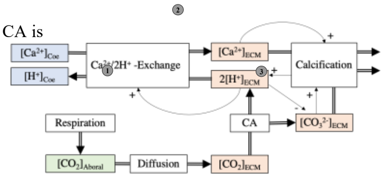

Light Enhanced Calcification

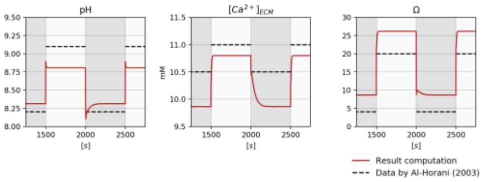

Light Enhanced Calcification

- Conclusion
  - We can reproduce the dynamics corresponding to the light and dark conditions, as were observed in literature (e. g. Al Horani 2003)
  - Simulated results were close to observed data as reported in literature, but not exactly the same.
  - Other hypotheses, such as bicarbonate transporters, might play an important role in obtaining these exact results and should be explored in upcoming research.

Overall conclusion

- We can create a simple spatial model that analyzed the chemical composition of the ECM.
- The model contained at least one steady state value with biological relevant concentrations of TA and DIC.
- This steady state is strongly dependent on the respiration rate in the Calicoblastic cells.
- This steady state is strongly dependent on the concentration of Carbonic Anhydrase in the ECM.
- Using these correlations, we were able to reproduce light and dark dynamics are caused by LEC.

Further research

- One of the shortcomings of this model is that the respiration rate and Ca^{2+}-ATPase are chosen by the researcher and do not follow from the available energy and O_2.
- Expanding the topology of the model, including the photosynthesis in the oral layer, would allow such an internal energy calculation.
- An expanded model could possibly reproduce spatial data from sites other than the ECM, such as the surface and coelenteron.
- This would also make the model potentially suitable to predict O_2 production and impact on coral bleaching.

References

- 1. Al-Horani, F.A., Al-Moghrabi, S.M. & de Beer, D. The mechanism of calcification and its relation to photosynthesis and respiration in the scleractinian coral *Galaxea fascicularis* . *Marine Biology* **142,** 419–426 (2003). https://doi.org/10.1007/s00227-002-0981-8
- 2. Taubner, Isabelle & Hu, Marian & Eisenhauer, Anton & Bleich, Markus. (2019). Electrophysiological evidence for light-activated cation transport in calcifying corals. Proceedings of the Royal Society B: Biological Sciences. 286. 20182444. 10.1098/rspb.2018.2444.
- 3. Nakamura, Takashi & Nadaoka, Kazuo & Watanabe, Atsushi. (2013). A coral polyp model of photosynthesis, respiration and calcification incorporating a transcellular ion transport mechanism. Coral Reefs. 32. 10.1007/s00338-013-1032-2.
- 4. Eyal, Gal & Cohen, Itay & Eyal-Shaham, Lee & Ben-Zvi, Or & Tikochinski, Yaron & Loya, Yossi. (2019). Photoacclimation and induction of light-enhanced calcification in the mesophotic coral Euphyllia paradivisa. Royal Society Open Science. 6. 180527. 10.1098/rsos.180527.
- 5. Allemand, Denis & Ferrier-Pagès, Christine & Furla, Paola & Houlbreque, Fanny & Puverel, Sandrine & Reynaud, Stéphanie & Tambutté, Eric & Tambutté, Sylvie & Zoccola, Didier. (2004). Biomineralisation in reef-building corals: From molecular mechanisms to environmental control. Comptes Rendus Palevol. 3. 453-467. 10.1016/j.crpv.2004.07.011.
- 6. Zoccola, Didier & Ganot, Philippe & Bertucci, Anthony & Segonds, Natacha & Techer, Nathalie & Voolstra, Christian & Aranda Lastra, Manuel & Tambutté, Eric & Allemand, Denis & Casey, Joseph & Tambutté, Sylvie. (2015). Bicarbonate transporters in corals point towards a key step in the evolution of Cnidarian calcification. Scientific Reports. 5. 9983. 10.1038/srep09983.
- 7. Moya, Aurelie & Tambutté, Sylvie & Bertucci, Anthony & Tambutté, Eric & Lotto, Séverine & Vullo, Daniela & Supuran, Claudiu & Allemand, Denis & Zoccola, Didier. (2008). Carbonic Anhydrase in the Scleractinian Coral Stylophora pistillata. The Journal of biological chemistry. 283. 25475-84. 10.1074/jbc.M804726200.

References

- 8. Bertucci, Anthony & Tambutté, Sylvie & Supuran, Claudiu & Allemand, Denis & Zoccola, Didier. (2011). A New Coral Carbonic Anhydrase in Stylophora pistillata. Marine biotechnology (New York, N.Y.). 13. 992-1002. 10.1007/s10126-011-9363-x.
- 9. Beschrijven vesticles ACC amorphous calcium carbonate Sun, Chang-Yu & Stifler, Cayla & Chopdekar, Rajesh & Schmidt, Connor & Parida, Ganesh & Schoeppler, Vanessa & Fordyce, Benjamin & Brau, Jack & Mass, Tali & Tambutté, Sylvie & Gilbert, Pupa. (2020). From particle attachment to space-filling coral skeletons. Proceedings of the National Academy of Sciences. 117. 10.1073/pnas.2012025117.
- 10. Yuan, Xiangcheng & Cai, Wei-Jun & Meile, Christof & Hopkinson, Brian & Ding, Qian & Schoepf, Verena & Warner, Mark & Hoadley, Kenneth & Chen, Bingzhang & Liu, Sheng & Huang, Hui & Ying, Ye & Grottoli, Andrea. (2018). Quantitative interpretation of vertical profiles of calcium and pH in the coral coelenteron. Marine Chemistry. 204. 10.1016/j.marchem.2018.06.001.
- 11. Raybaud, Virginie & Tambutté, Sylvie & Ferrier-Pagès, Christine & Reynaud, Stéphanie & Venn, Alexander & Tambutté, Eric & Nival, Paul & Allemand, Denis. (2017). Computing the carbonate chemistry of the coral calcifying medium and its response to ocean acidification. Journal of Theoretical Biology. 424. 10.1016/j.jtbi.2017.04.028.
- 12. Orr, James & Epitalon, Jean-Marie & Gattuso, Jean-Pierre. (2015). Comparison of ten packages that compute ocean carbonate chemistry. Biogeosciences. 12. 1483-1510. 10.5194/bg-12-1483-2015.
- 13. Zeebe, Richard & Wolf-Gladrow, Dieter. (2001). CO2 in Seawater: Equilibrium, kinetics, isotopes.
- 14. Tambutté E, Tambutté S, Segonds N, Zoccola D, Venn A, Erez J, et al. Calcein labelling and electrophysiology: insights on coral tissue permeability and calcification. Proc R Soc B Biol Sci. 2012;279(1726):19–27.
- 15. D'Olivo, J.P., McCulloch, M.T. Response of coral calcification and calcifying fluid composition to thermally induced bleaching stress. *Sci Rep* **7,** 2207 (2017). https://doi.org/10.1038/s41598-017-02306-x

Modelling the influence of the physical environment (hydrodynamics, light, temperature, Dissolved Inorganic Carbon) on calcification

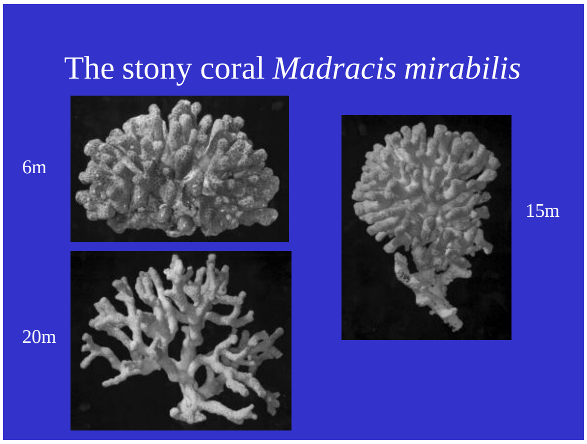

The stony coral *Madracis mirabilis*

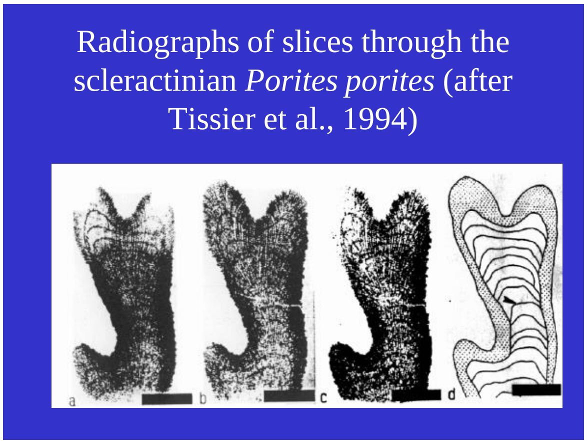

Radiographs of slices through the scleractinian *Porites porites* (after Tissier et al., 1994)

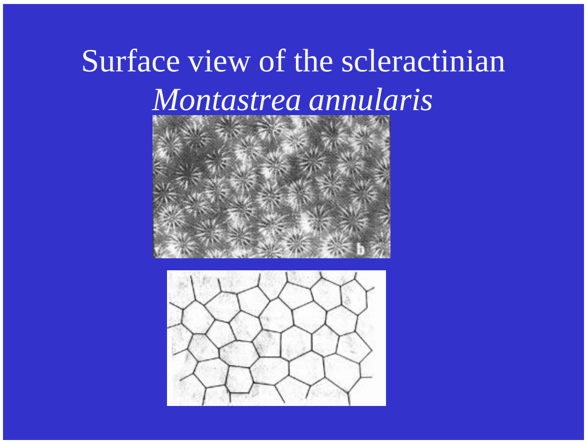

Surface view of the scleractinian *Montastrea annularis*

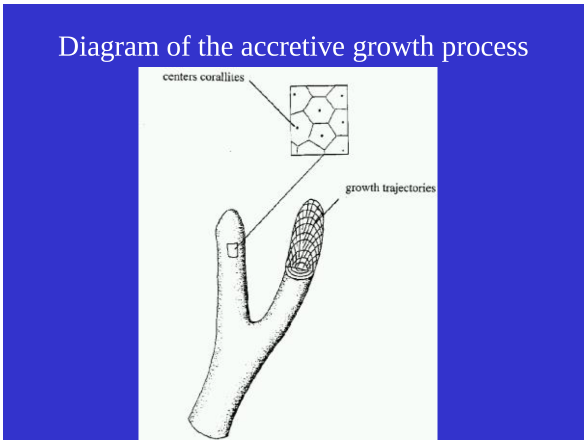

Diagram of the accretive growth process

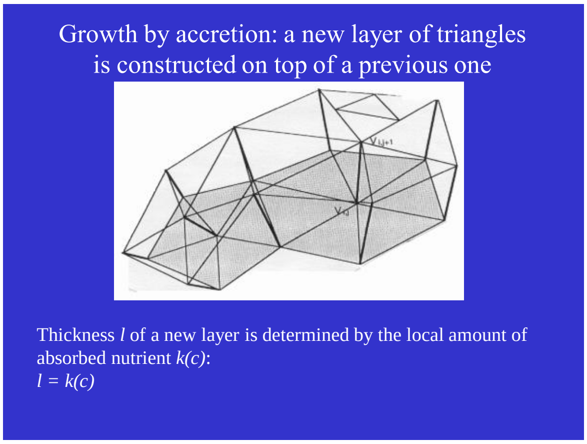

Growth by accretion: a new layer of triangles is constructed on top of a previous one

Thickness *l* of a new layer is determined by the local amount of absorbed nutrient *k(c)*:
$l = k(c)$

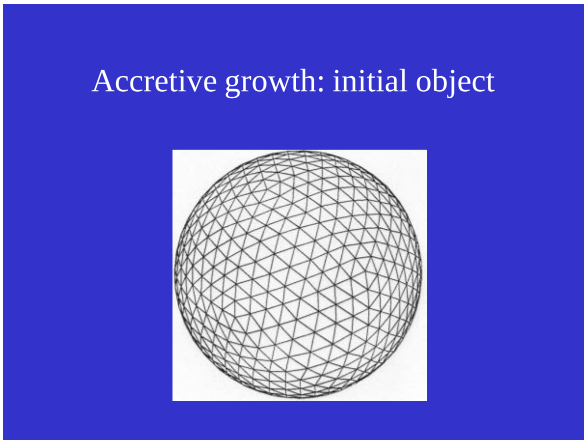

Accretive growth: initial object

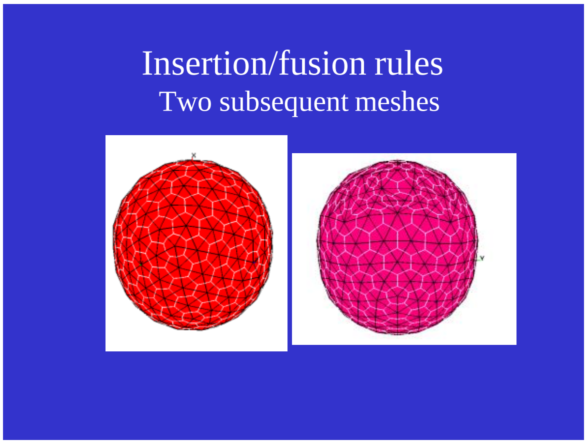

Insertion/fusion rules

Two subsequent meshes

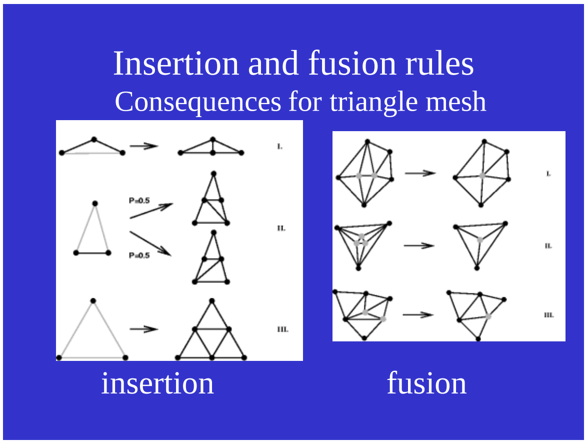

Insertion and fusion rules

Consequences for triangle mesh

insertion fusion

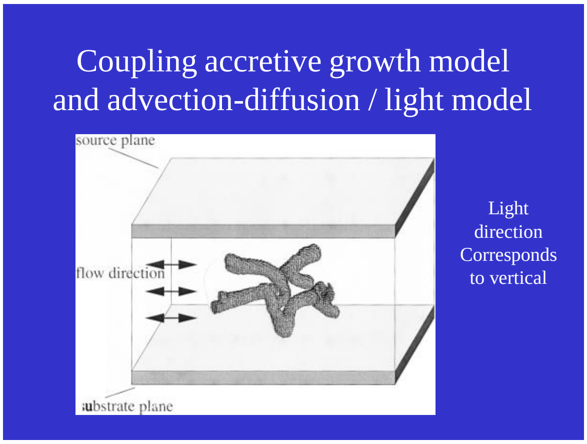

Coupling accretive growth model and advection-diffusion / light model

Light direction Corresponds to vertical

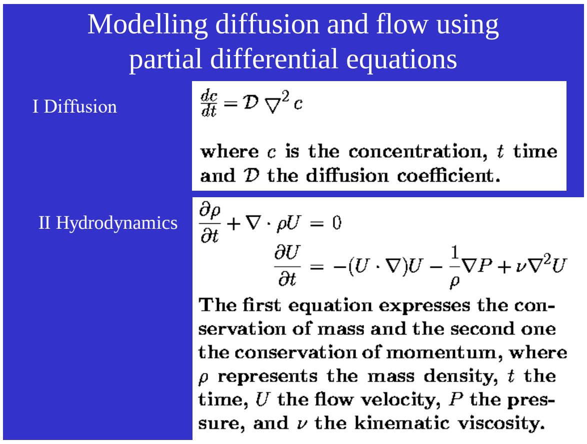

Modelling diffusion and flow using partial differential equations

I Diffusion

$$\frac{dc}{dt} = \mathcal{D}\,\nabla^2 c$$

where c is the concentration, t time and $\mathcal{D}$ the diffusion coefficient.

II Hydrodynamics

$$\frac{\partial\rho}{\partial t} + \nabla\cdot\rho U = 0$$

$$\frac{\partial U}{\partial t} = -(U\cdot\nabla)U - \frac{1}{\rho}\nabla P + \nu\nabla^2 U$$

The first equation expresses the conservation of mass and the second one the conservation of momentum, where ρ represents the mass density, t the time, U the flow velocity, P the pressure, and ν the kinematic viscosity.

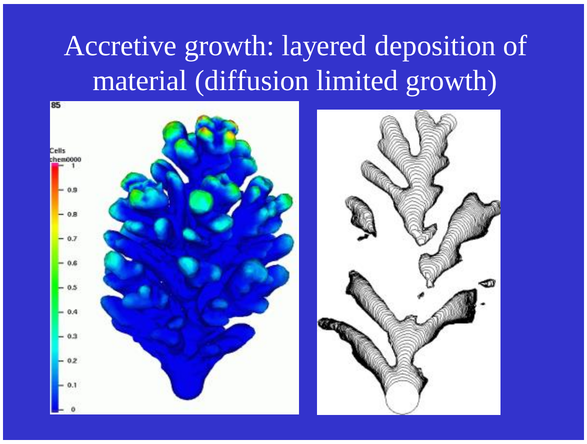

Accretive growth: layered deposition of material (diffusion limited growth)

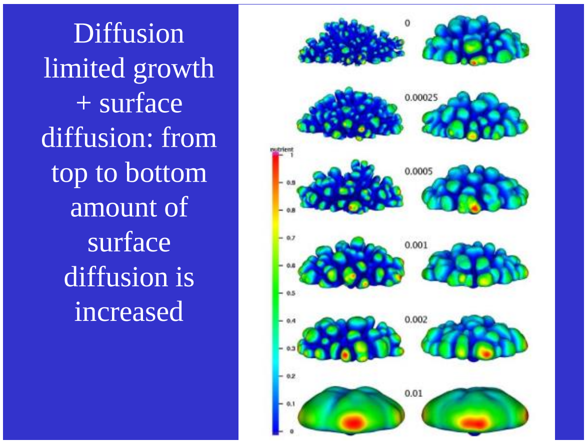

Diffusion limited growth + surface diffusion: from top to bottom amount of surface diffusion is increased

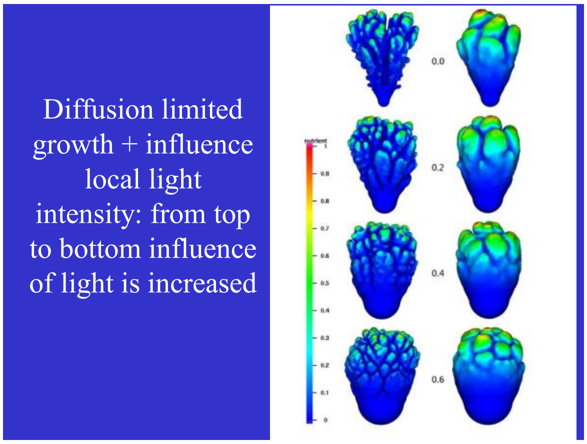

Diffusion limited growth + influence local light intensity: from top to bottom influence of light is increased

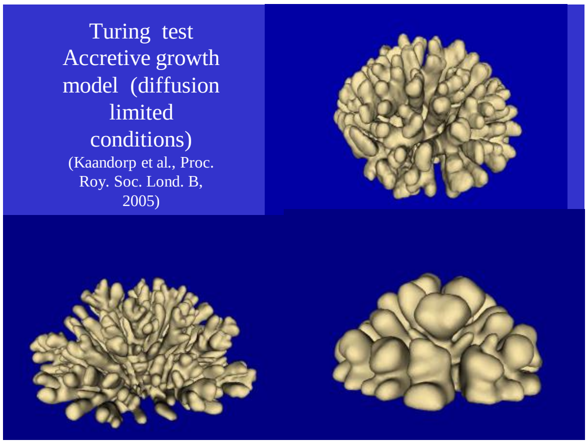

Turing test Accretive growth model (diffusion limited conditions)
(Kaandorp et al., Proc. Roy. Soc. Lond. B, 2005)

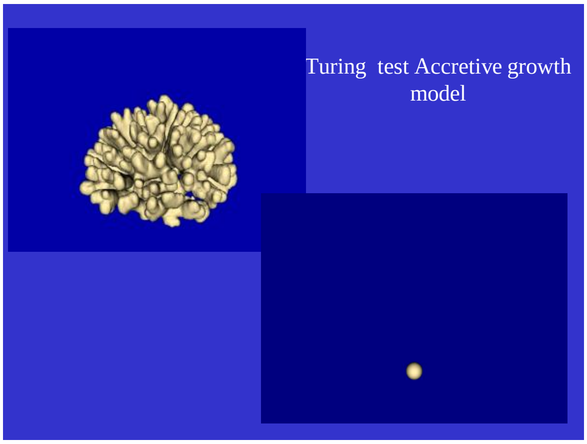

Turing test Accretive growth model

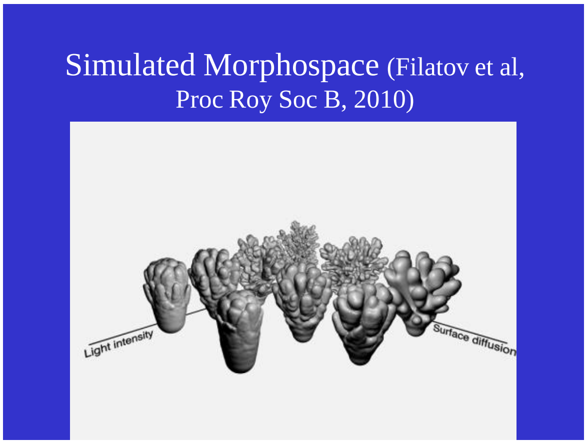

Simulated Morphospace (Filatov et al, Proc Roy Soc B, 2010)

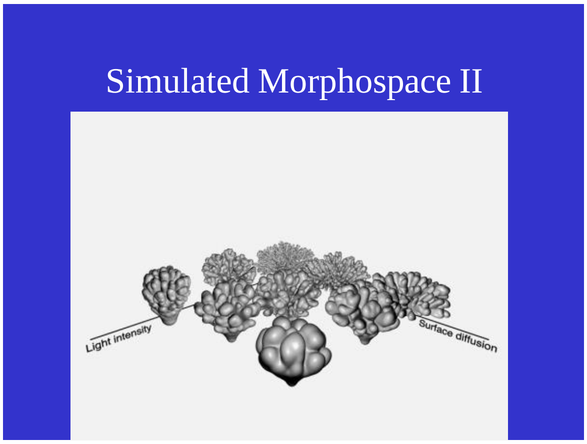

Simulated Morphospace II

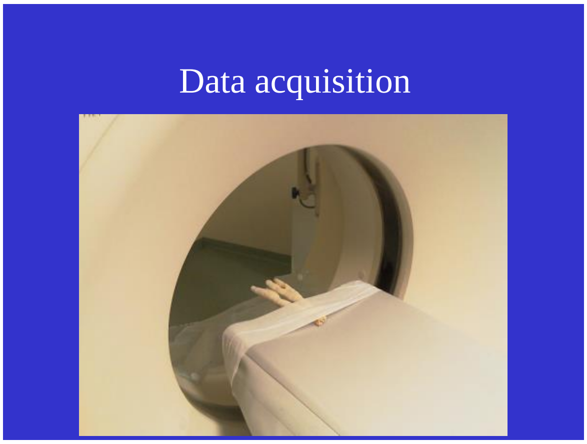

Data acquisition

Comparison morphologies in different *Madracis* species

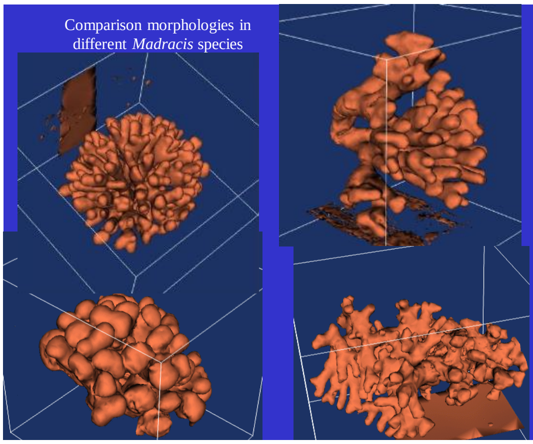

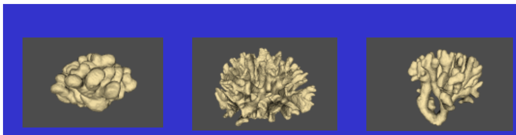

- Samples (CT-scans) of 4 coral species
  - *Madracis decactis*
  - *Madracis mirabilis*
  - *Madracis carmabi*
  - *Madracis formosa*

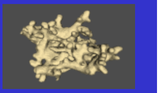

Data processing

- DICOM image processing (e.g. filtering)
- Iso-surface extraction
- 3D-volume construction

Landmark-based methods in unitary organisms (D'Arcy Thompson, 1917)

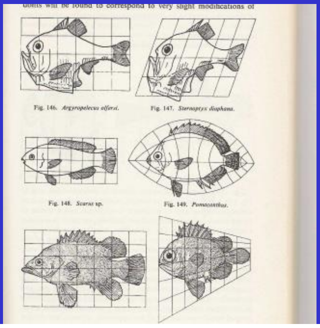

Morphometrics of 3D indeterminate (branching) growth forms

- Global measurements: fractal dimensions,branch ordening, compactness, surface, volume, surface/volume
- Local measurements: local curvature and morphological skeletons in 3D

Morphological Skeleton in a 3D images of the coral *Madracis mirabilis* (K. Kruszynski, J.A. Kaandorp, R. van Liere, Coral Reefs 2007)

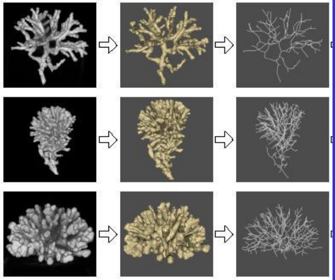

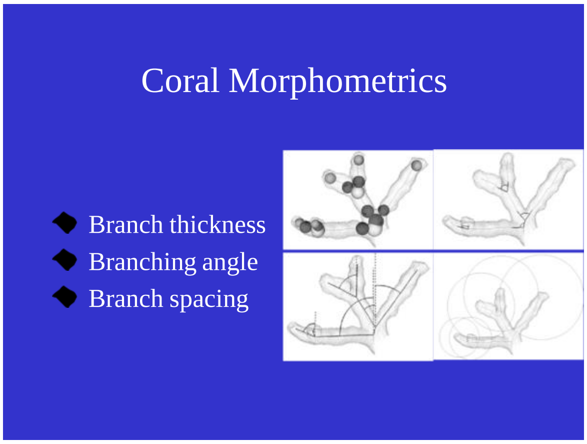

Coral Morphometrics

- Branch thickness
- Branching angle
- Branch spacing

91

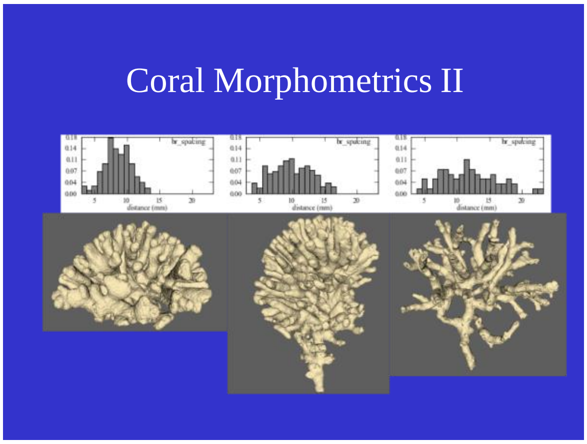

Coral Morphometrics II

92

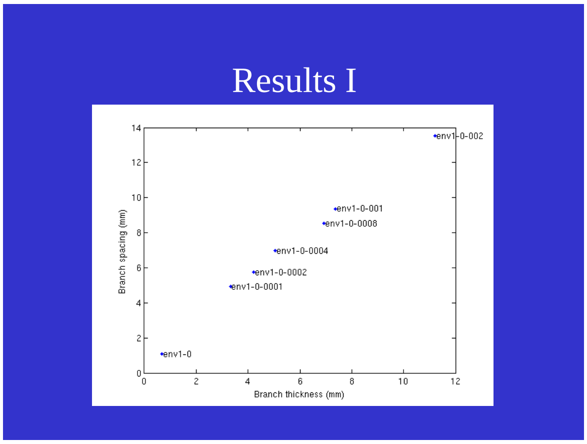

Results I

93

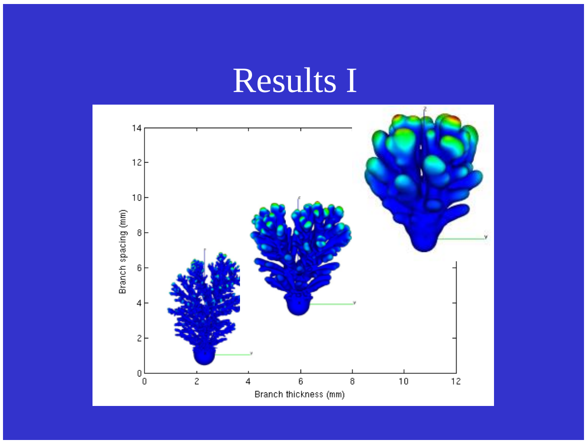

Results I

94

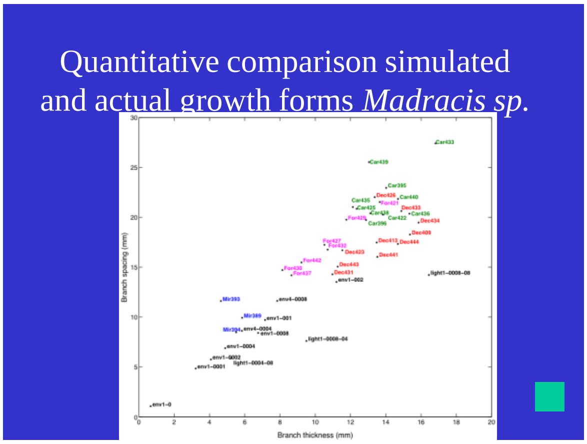

Quantitative comparison simulated and actual growth forms *Madracis sp.*

95

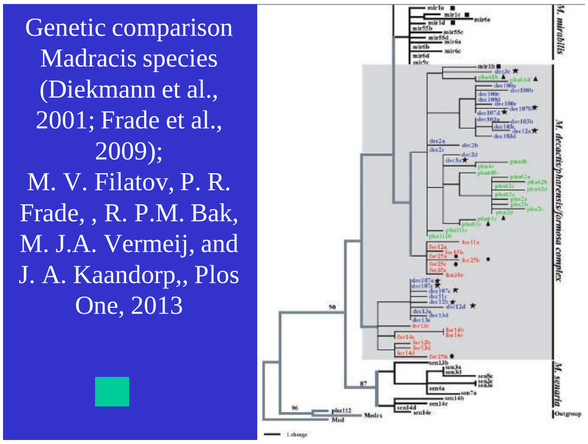

Genetic comparison Madracis species (Diekmann et al., 2001; Frade et al., 2009);
M. V. Filatov, P. R. Frade, , R. P.M. Bak, M. J.A. Vermeij, and J. A. Kaandorp,, Plos One, 2013

96

Specific combination of 3D-based measures aids species delimitation in irregularly shaped and taxonomically challenging marine taxa ***(submitted)***

Catalina Ramírez-Portilla, Inge Bieger, Robert G. Belleman, Thomas Wilke, Jean-François Flot, Andrew H. Baird, Saki Harii, Frederic Sinniger, Jaap Kaanorp

Acropora digitifera low flow morphology

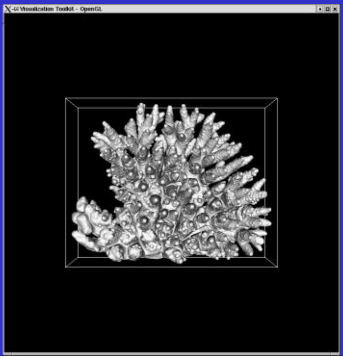

Acropora digitifera high flow morphology

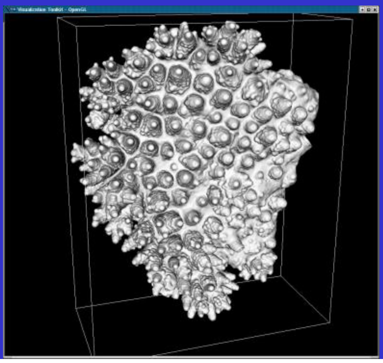

Survival of *Acropora digitifera* for high and low flow velocities (Nakamura & van Woesik, 2001)

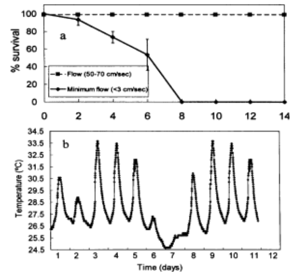

Figure 2. Percent survival (a)of *Acropora digitifera* at elevated temperatures(b) while maintained under high (50-70 cm/sec) and low (<3 cm/sec) flow (Nakamura & Van Woesik 2001).

Develop quantitative measures to characterize morphology using high resolution polygon meshes from three closely related *Acropora (A.)* species *(C. Ramirez-Portilla, I Bieger et al., submitted)*:

- ***A.* cf. *bifurcata***
- ***A.* cf. *cytherea***
- ***A.* aff. *hyacinthus***

Which 3D-derived metrics can aid to delineate these species?

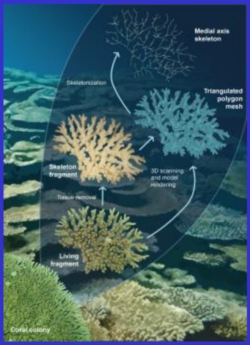

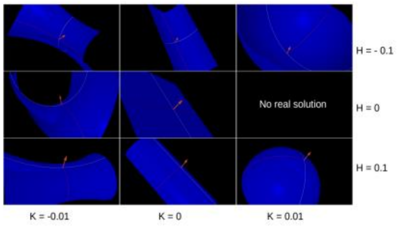

Curvature of a surface
k_1 : maximum curvature
k_2 : minimum curvature
Mean (H) curvature:

$H = (k_1 + k_2)/2$

Gaussian (K) curvature: $K = k_1 * k_2$

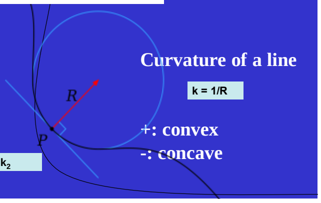

Curvature of a line

$k = 1/R$

+: convex
-: concave

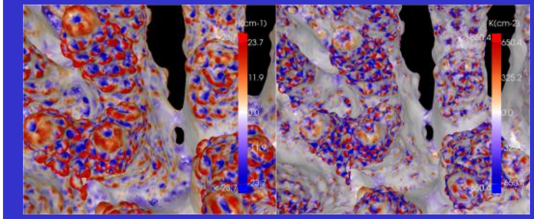

Pictures by Andrew H. Baird

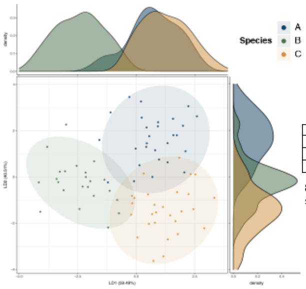

Linear discriminant analysis (LDA)

LDA	Allocated to A	Allocated to B	Allocated to C
A	23	2	3
B	0	22	1
C	2	0	26

89.87% of discriminative power (71/79 specimens)

Modelling the influence of the physical environment II (hydrodynamics, light, temperature, Dissolved Inorganic Carbon) on calcification

- N. Chindapol , J. A. Kaandorp , C. Cronemberger, T. Mass and A. Genin PLOS Computational Biology, 9, e1002849, 2013

Research Question

- Is morphological plasticity in corals genetically controlled or influenced by external factors? Accretive growth model is used to investigate the phenotypic response of the growth of simulated coral under the influence of ***uni-directional*** current.

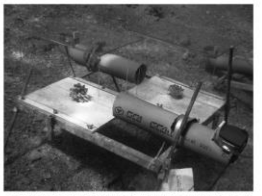

Fig. 1. Underwater setup of flow-manipulation experiment showing 2 units each consisting of a transparent, upside down U-shape box (40 × 40 × 30 cm) and a pump attached to a 50 cm long, 10.1 cm diameter pipe directed at the coral

Mass et al., 2010

Research Questions

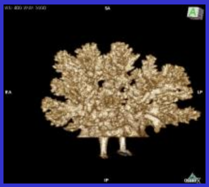

CT scan *Pocillopora verrucosa* (from experiment by Mass & Genin 08.)

- **Research question 1**: Is the symmetry found in coral colony determined by symmetry in the flow rather than intrinsic control by the coral?
- **Research question 2**: Is a local increase of O2 concentrations produced by photosynthesis the cause of bleaching under low flow conditions?

Modelling diffusion and flow using partial differential equations

I Diffusion

$$\frac{dc}{dt} = \mathcal{D}\,\nabla^2 c$$

where c is the concentration, t time and $\mathcal{D}$ the diffusion coefficient.

II Hydrodynamics

$$\frac{\partial \rho}{\partial t} + \nabla \cdot \rho U = 0$$

$$\frac{\partial U}{\partial t} = -(U \cdot \nabla)U - \frac{1}{\rho}\nabla P + \nu \nabla^2 U$$

The first equation expresses the conservation of mass and the second one the conservation of momentum, where ρ represents the mass density, t the time, U the flow velocity, P the pressure, and ν the kinematic viscosity.

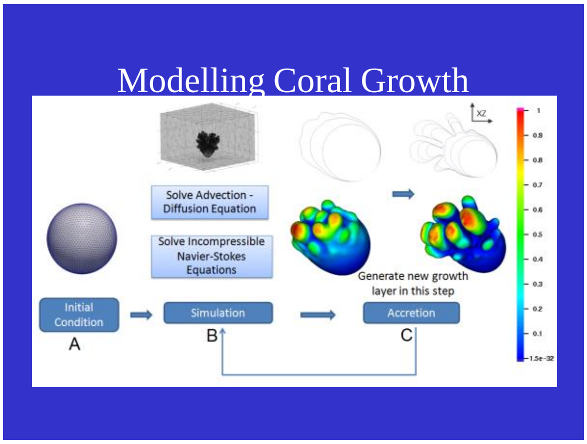

Modelling Coral Growth

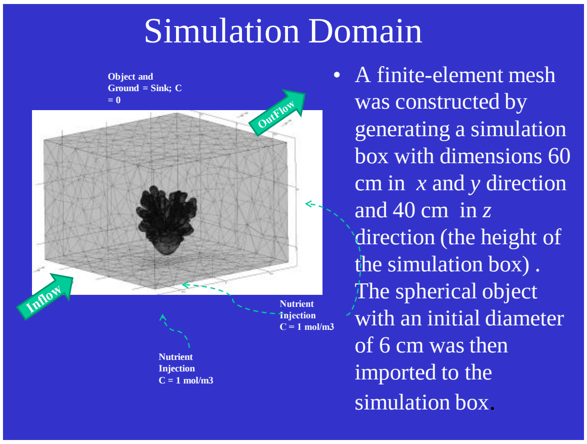

Simulation Domain

- A finite-element mesh was constructed by generating a simulation box with dimensions 60 cm in *x* and *y* direction and 40 cm in *z* direction (the height of the simulation box) . The spherical object with an initial diameter of 6 cm was then imported to the simulation box.

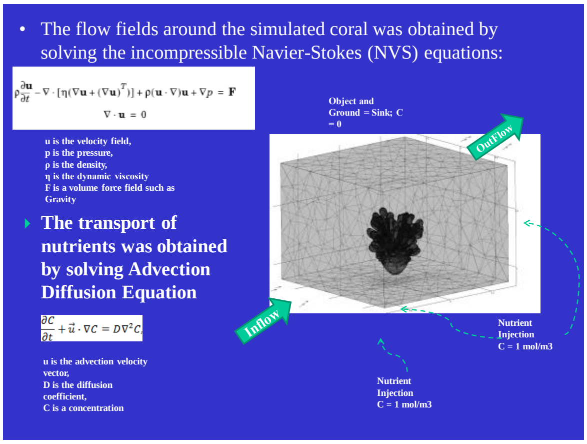

- The flow fields around the simulated coral was obtained by solving the incompressible Navier-Stokes (NVS) equations:

$$\rho\frac{\partial \mathbf{u}}{\partial t} - \nabla \cdot [\eta(\nabla \mathbf{u} + (\nabla \mathbf{u})^T)] + \rho(\mathbf{u} \cdot \nabla)\mathbf{u} + \nabla p = \mathbf{F}$$

$$\nabla \cdot \mathbf{u} = 0$$

u is the velocity field,
p is the pressure,
ρ is the density,
η is the dynamic viscosity
F is a volume force field such as Gravity

- **The transport of nutrients was obtained by solving Advection Diffusion Equation**

$$\frac{\partial C}{\partial t} + \vec{u} \cdot \nabla C = D\nabla^2 C,$$

u is the advection velocity vector,
D is the diffusion coefficient,
C is a concentration

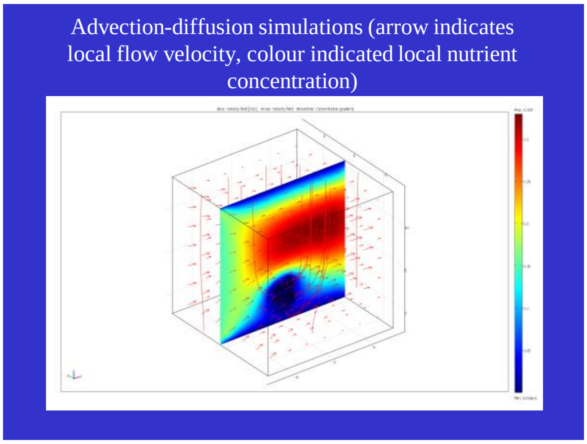

Advection-diffusion simulations (arrow indicates local flow velocity, colour indicated local nutrient concentration)

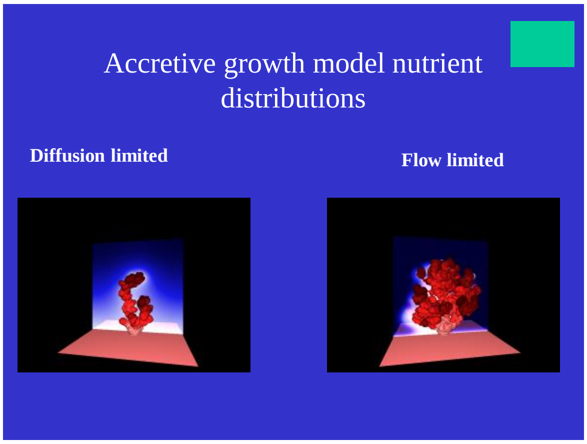

Accretive growth model nutrient distributions

Diffusion limited

Flow limited

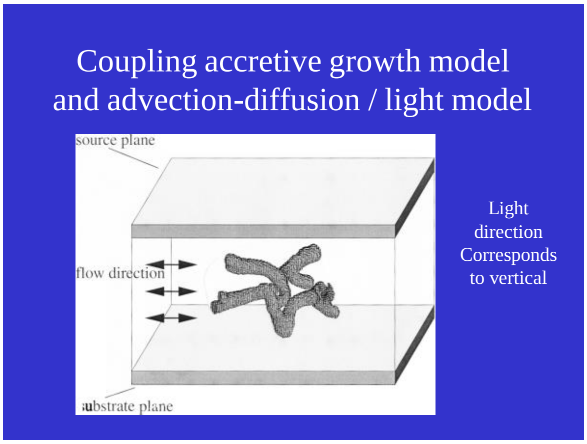

Coupling accretive growth model and advection-diffusion / light model

Light direction Corresponds to vertical

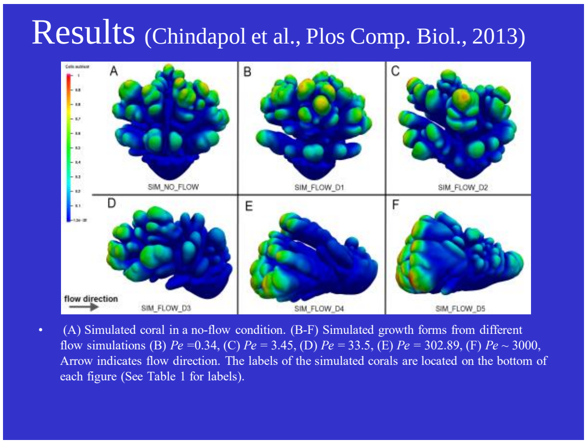

Results (Chindapol et al., Plos Comp. Biol., 2013)

- (A) Simulated coral in a no-flow condition. (B-F) Simulated growth forms from different flow simulations (B) *Pe* =0.34, (C) *Pe* = 3.45, (D) *Pe* = 33.5, (E) *Pe* = 302.89, (F) *Pe* ~ 3000, Arrow indicates flow direction. The labels of the simulated corals are located on the bottom of each figure (See Table 1 for labels).

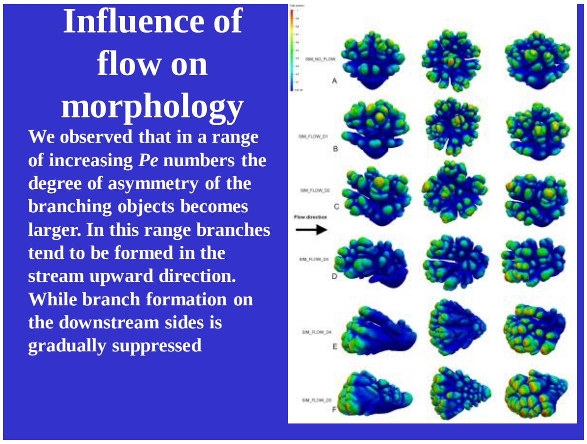

Influence of flow on morphology

We observed that in a range of increasing *Pe* numbers the degree of asymmetry of the branching objects becomes larger. In this range branches tend to be formed in the stream upward direction. While branch formation on the downstream sides is gradually suppressed

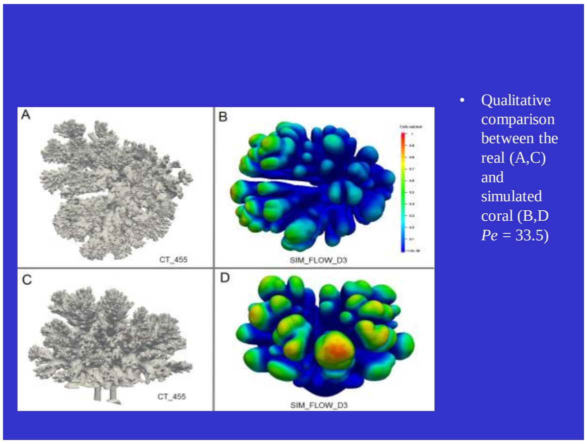

- Qualitative comparison between the real (A,C) and simulated coral (B,D *Pe* = 33.5)

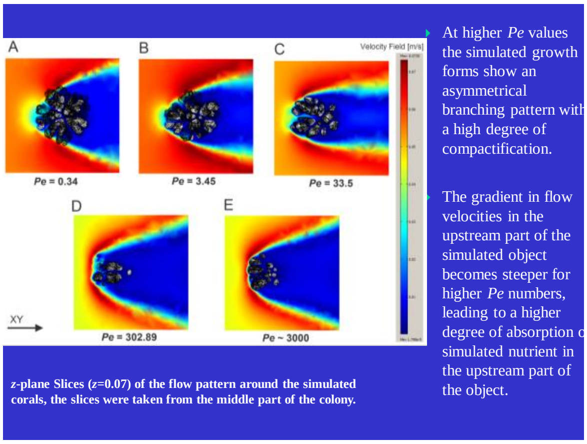

z-plane Slices (*z*=0.07) of the flow pattern around the simulated corals, the slices were taken from the middle part of the colony.

- At higher *Pe* values the simulated growth forms show an asymmetrical branching pattern with a high degree of compactification.
- The gradient in flow velocities in the upstream part of the simulated object becomes steeper for higher *Pe* numbers, leading to a higher degree of absorption o simulated nutrient in the upstream part of the object.

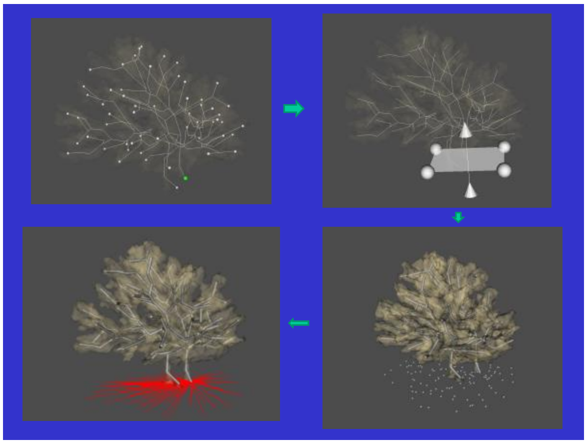

A single value approximation of the symmetry

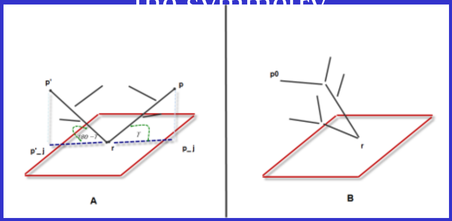

Symmetry of the coral colony can be simplified by using the sum of all projected endpoints or bifurcation points. Let's p be an arbitrary point in the skeleton graph, brach rp is considered to be perfectly symmetric if and only if there exist another branch rp' such that sum of their projection is equal to zero. The symmetry of the coral colony therefore is a result of the sum of either endpoint (endpoint symmetry) or all point including bifurcation point (colony symmetry)

Quantification of the impact of flow on the symmetry of branching growth forms

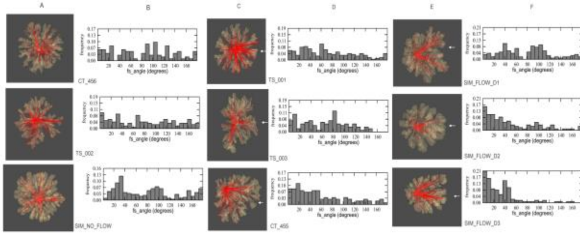

- When comparing the *fs_angle* in the histograms for increasing *Pe* numbers, we can observe that the *fs_angle* is more or less evenly distributed for low *Pe* values, while for increasing *Pe* numbers the distribution becomes more skewed and the degree of asymmetry of the branching form increases. The skewness of the distributions in these histograms can be used to quantify the degree of asymmetry of the different growth forms
-

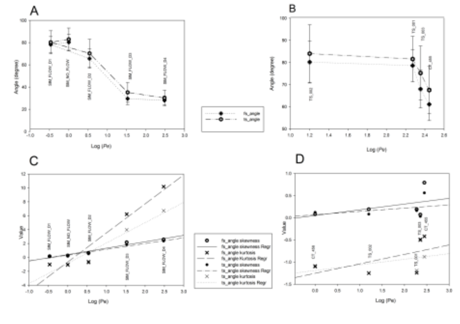

- (A-B) Mean value of *fs_angle* and *ts_angle* plot against *Pe* value for both simulated forms and real corals. Error bars indicate 95% confidence interval. (C-D) Regression plot of skewness and kurtosis against Pe value for both simulated forms and real corals

Conclusion

- Increasing the *Pe* number induces the formation of asymmetrical branching growth forms
- In the flow simulations, we have found a decreasing trend of the surface/volume ratio and increased skewedness which is the same as real corals
- Our model shows that in this case there is no gene regulation needed to explain the formation of asymmetrical branching forms
- In reality most scleractinian corals will not be growing under uni-directional flow conditions but will be exposed to a two-phase flow where the flow direction is reversing twice a day because of the tidal movements.

Conclusions and Open Questions

- Many crucial parts of information are still missing, there are many gaps in the knowledge of molecular biology and the physiology of calcification
- Many (Most) details about gene regulation of calcification are missing
- The genome of a scleractinian coral and its symbiont are available, important for research on gene regulation of calcification
- How are gene expression in the host (the coral) and symbiont related is not very well known
- Models can be used to infer regulatory networks from gene expression data, understand the fluxes in complicated metabolic pathways, study the influence of the physical environment in detail, to study how the different processes at very different scales in time and space are coupled
- Models can be used to organize data and data collection and to detect the missing pieces of knowledge in a systematic way

Acknowledgements

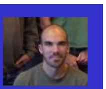

Carlos Tamulonis

Daniel Botman

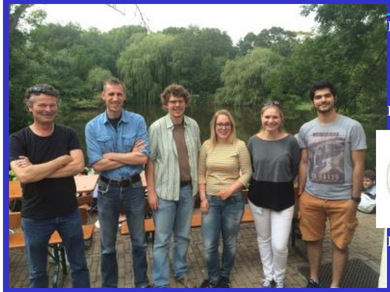

Imke Lansky

Paula Ramos-Silva

Helena Willard

Maarten van der Sande

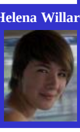

Roland Dries, Fredrik Jansson, Johanna Gronqvist, Eva Deutekom and Amir Abdol

Inge Bieger

Catalina Ramirez

Acknowledgements

- Stefano Goffredo and Giuseppe Falini, University of Bologna, Italy
- Eric Rottinger, Université Nice Sophia Antipolis, Institute for Research on Cancer and Aging, Nice, France
- Evelyn Houliston, Villefranch-sur-mer; Lab developmental Biology, France
- Mark Q. Martindale, Whitney Lab for Marine Bioscience, University of Florida, St. Augustine, Florida, USA
- Yulia Kraus, Moscow State University, Russia
- Jorg Hammel, University of Jena, Germany
- Grisha Genikhovich, University of Austria

On concretions, spicules, and specular skeletons (Ch IX, D’Arcy Thompson, 1945)

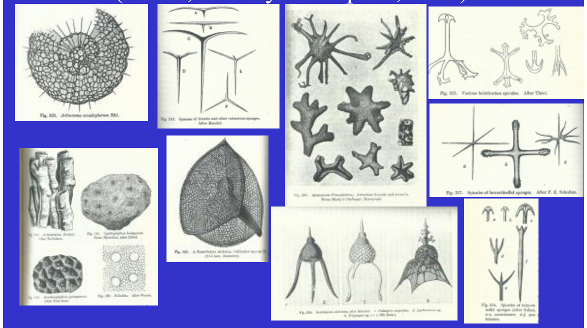

References

- D. Allemand et al., Biomineralisation in reef-building corals: from molecular mechanisms to environmental control, C.R. Palevol 3:453,2004
- G. Death, J.M.Lough, K. Fabricius, Declining coral calcification on the Great Barrier Reef, Science 323:116, 2009
- M.V. Filatov, J.A. Kaandorp, M. Postma, R. van Liere, K.J. Kruszynski, M.J.A. Vermeij, G.J. Streekstra and R.P.M.Bak, A comparison between coral colonies from the Madracis genus and simulated forms, Proc. R. Soc. B 277:3555-3561, 2010
- Y. Fomekong Nanfack, J.A. Kaandorp and J.G. Blom Efficient parameter estimation for spatio-temporal models of pattern formation: Case study of *Drosophila melanogaster* Bioinformatics 23:3356-3363, 2007
- J.P. Gattuso, Ocean acidification, Encyclopedia of Earth, 2008, http://www.eoearth.org/article/Ocean_acidification
- J.A. Kaandorp, P.M.A. Sloot, R.M.H. Merks, R.P.M. Bak, M.J.A. Vermeij, and C. Maier Morphogenesis of the branching reef coral Madracis mirabilis, Proc. Roy. Soc. B. 272:127-133, 2005
- Moya A, Huisman L, Ball EE, Hayward DC, Grasso LC, Chua CM, Woo HN, Gattuso JP, Forêt S, Miller DJ.,, Whole transcriptome analysis of the coral Acropora millepora reveals complex responses to CO_2-driven acidification during the initiation of calcification, , Mol Ecol. 2012 May;21(10):2440-54
- C. Tamulonis, M. Postma, H. Marlow, C. Magie, J. de Jong and J.A. Kaandorp, Morphometrics & Modeling of *Nematostella vectensis* Gastrulation, Developmental Biology 351:217-228, 2011
- K. Kruszynski, J.A. Kaandorp and R. van Liere A computational method for quantifying morphological variation in scleractinian corals, Coral Reefs 26:831-840, 2007
- N. Leqlerq, J.P. Gattuso, J. Jaubert, CO2 partial pressure controls the calcification rate of a coral community, Global Change 6:329, 2000
- Coral Bleaching: lecture by Madeleine van Oppen, AUSTRALIAN FRONTIERS OF SCIENCE, 2005, Walter and Eliza Hall Institute of Medical Research, Melbourne, 12-13 April 2005 *Molecular ecology of the coral-algal symbiosis*
- V.M. Weis, D. Allemand, What determines coral health, Science, 324: 1153, 2009
- Charly Veron’s lecture for the Royal Society on June 2009: https://www.zsl.org/science/news/join-our-campaign-to-save-the-worlds-coral,1209,AR.html
- Wikipedia, Ocean acidification

D. Botman and J.A. Kaandorp, Spatial gene expression quantification: a tool for analysis of in situ hybridizations in sea anemone Nematostella vectensis,. BMC Research Notes 5:555, 2012

N. Chindapol , J. A. Kaandorp , C. Cronemberger, T. Mass and A. Genin Modelling growth and form of the scleractinian coral *Pocillopora verrucosa* and the influence of hydrodynamics, PLOS Computational Biology, 9, e1002849, 2013

P. Ramos-Silva, F. Marin, J.A. Kaandorp, and B. Marie, « Biomineralization toolkit »: the importance of sample cleaning prior to the characterization of biomineral proteomes, PNAS ., 3–5. doi:10.1073/pnas.1303657110, 2013

P. Ramos-Silva J.A, Kaandorp, L. Huisman, B. Marie, I. Zanella-Cléon4, N. Guichard, D.J. Miller and F. Marin, The skeletal proteome of the coral Acropora millepora: the evolution of calcification by cooption and domain shuffling, Molecular Biology and Evolution, 30:2099-2112, 2013 http//mbe.oxfordjournals.org/content/early/2013/06/12/molbev.mst109.full.pdf 2013

J. Tanzil, Jani; B. Brown, R. Dunne, L. Jen Nie; J.A. Kaandorp, and P. Todd, Regional decline in growth rates of massive Porites corals in Southeast Asia, Global Change Biology, 19:3011-3023, 2013

M. V. Filatov, P. R. Frade, , R. P.M. Bak, M. J.A. Vermeij, and J. A. Kaandorp, Comparison between colony morphology and molecular phylogeny in the Caribbean scleractinian coral genus Madracis, Plos One Plos One 8, e71287, 2013

Ramos-Silva, P., Kaandorp, J., Marin, F., et al. The skeleton of the staghorn coral *Acropora millepora*: a molecular and structural characterization, Plos One, 01/2014; 9(6):e97454. DOI: 10.1371/journal.pone.0097454

D. Botman, E. Rottinger, M. Q. Martindale, J. de Jong and J. A. Kaandorp, Computational Approach towards a Gene Regulatory Network for the Developing Nematostella vectensis Gut., Plos One, 9: e103341, 2014

P. Fantazzini, S. Mengoli, L. Pasquini, V. Bortolotti, L. Brizi1, M. Mariani, M. Di Giosia, S. Fermani, B. Capaccioni, E. Caroselli, F. Prada, F. Zaccanti, O. Levy, Z. Dubinsky, J. A. Kaandorp, P. Konglerd, J. U. Hammel, Y. Dauphin, J. Cuif, J. C. Weaver, K. E. Fabricius, W. Wagermaier, P. Fratzl, G. Falini and S. Goffredo, Gains and losses of coral skeletal porosity changes with ocean acidification acclimation, Nature Communications, DOI: 10.1038/ncomms8785, 2015

D. Botman; F. Jansson; E. Röttinger; M. Q. Martindale; J. de Jong; J.A. Kaandorp Analysis of a spatial gene expression database for sea anemone Nematostella vectensis during early development BMC Systems Biology 9::63, 2015

J. Tanzil , J.N. Lee , B.E. Brown, R. Quax, J.A. Kaandorp , J.M. Lough , P.A. Todd. Luminescence and density banding patterns in massive Porites corals around the Thai-Malay Peninsula, Southeast Asia, Limnology & Oceanography, doi: 10.1002/lno.1035, 2016

Amir M Abdol, Eric Röttinger, Fredrik Jansson, Jaap A Kaandorp, A novel technique to combine and analyse spatial and temporal expression datasets: A case study with the sea anemone *Nematostella vectensis* to identify potential gene interactions, Developmental biology, 428:204-214, 2017

A.M.Abdol A. Bedard, I. Lánský, J.A.Kaandorp, High-throughput method *for* extracting and visualizing the spatial gene expressions from in situ hybridization images: A case study of the early development of the sea anemone *Nematostella vectensis*, Gene Expression Patterns 27:36-45, 2018

A.M. Abdol, D. Cicin-Sain, J. A Kaandorp, A. Crombach, Scatter Search Applied to the Inference of a Development Gene Network, Computation 5:22-, 2017, doi:10.3390/computation5020022

R.H Ong, A.J.C King, J.A Kaandorp, B.J. Mullins, M.J. Caley The effect of allometric scaling in coral thermal microenvironments PloS one 12 (10), e0184214, 2017

L Li, AJ Fijneman, JA Kaandorp, J Aizenberg, WL Noorduin Directed nucleation and growth by balancing local supersaturation and substrate/nucleus lattice mismatch Proceedings of the National Academy of Sciences 115 (14), 3575-3580, 2018 https://doi.org/10.1073/pnas.171291111

Yi Jin Liew, D. Zoccola, Yong Li, E. Tambutté, A. A. Venn, C. T. Michell1, Guoxin Cui1, E. S. Deutekom, J. A. Kaandorp, C. R. Voolstra, S. Forêt, D. Allemand, S. Tambutté, M. Aranda, Epigenome-associated phenotypic acclimatization to ocean acidification in a reef-building coral, Science Advances 4: eaar8028, 2018

Erik Caroselli , Francesca Gizzi , Fiorella Prada, Chiara Marchini , Valentina Airi , Jaap Kaandorp , Giuseppe Falini , Zvy Dubinsky, Stefano Goffredo, Low and variable pH decreases recruitment efficiency in populations of a temperate coral naturally present at a CO_2 vent, Limnology and Oceanography, 2018, https://doi.org/10.1002/lno.11097

Slavkov, D. Carrillo-Zapata, N. Carranza, X. Diego, F. Jansson, J. Kaandorp, S. Hauert, J. Sharpe, Morphogenesis in Robotic Swarms, Science Robotics, DOI: 10.1126/scirobotics.aau9178, 2018